From the Department of Medical Epidemiology and Biostatistics Karolinska Institutet, Stockholm, Sweden

Mathematical Model Development to Investigate the Pharmacokinetic Variability of Two Anticancer Drugs

Martin Fransson

Stockholm 2012

Published by Karolinska Institutet. Printed by Universitetsservice AB.

ISBN 978-91-7457-661-0

To my parents and brothers
- You are my role models

ABSTRACT

Pharmacokinetic variability in a population is the variability in plasma drug concentrations among individuals. It may, for instance, be caused by differences in genes coding for drug-transport proteins and metabolizing enzymes, amount of body fat, age, sex, patient compliance, diet or disease progression. For anticancer agents, the combination of a high variability and a narrow therapeutic window may cause adverse side events, with additional suffering for already afflicted patients and with high costs for society.

The work in this thesis aims to explore the possibilities for individualized treatment of two specific anticancer drugs, paclitaxel and imatinib, by developing mathematical models to investigate their pharmacokinetic variability.

In Paper I, two existing population pharmacokinetic models for paclitaxel are compared using a clinical study comprising thirty-three women treated for ovarian cancer. Using identifiability and sensitivity analysis, it is shown that a model describing the relation between total, unbound, and bound drug can be used with at least as good fit as a more empirical model, although only total plasma concentrations of paclitaxel are available.

In Paper II, the conclusions from Paper I are used to expand the mechanism-based model for paclitaxel to also include three metabolites. It is shown that the solubilizer Cremophor EL seems to have a strong effect on the kinetics of the two hydroxy-metabolites. Clearance of the main metabolite 6α-hydroxypaclitaxel (fraction metabolized) was significantly correlated ($p < 0.05$) with the ABCB1 allele G2677T/A. Individuals carrying the polymorphisms G/A ($n = 3$) or G/G ($n = 5$) showed a 30% increase, whereas individuals with polymorphism T/T ($n = 8$) showed a 27% decrease relative to those with the polymorphism G/T ($n = 17$).

In Paper III, a population pharmacokinetic model for imatinib is developed using data from a clinical study including fifty men and women on long-term treatment for gastrointestinal stromal tumour. It is shown that the pharmacokinetics is best described using a model with time dependent apparent bioavailability and absorption rate, which are decreased by approximately 30% and 50%, respectively, after three months of treatment. In addition, apparent clearance of imatinib was associated with the size of the liver metastasis, and was decreased by almost 4% for every 100 cm^3 of liver metastasis.

In Paper IV a semi-physiologically based pharmacokinetic model for paclitaxel and its metabolites is developed using existing models and data available in the literature. Sensitivity analysis of hepatic uptake, metabolism and efflux of the substances predicts systemic plasma concentrations of 6α-hydroxypaclitaxel to be sensitive to changes in the capacity of the ABCB1 transporter.

LIST OF PUBLICATIONS

This thesis is based on the following articles, which will be referred to in the text by their Roman numerals (I -IV):

I. Fransson M, Gréen H.
Comparison of two types of population pharmacokinetic model structures of paclitaxel.
European Journal of Pharmaceutical Sciences. 2008; 33(2):128-137

II. Fransson MN, Gréen H, Litton JE, Friberg LE.
Influence of Cremophor EL and genetic polymorphisms on the pharmacokinetics of paclitaxel and its metabolites using a mechanism-based model.
Drug Metabolism and Disposition. 2011; 39(2):247-255

III. Eechoute E, Fransson MN, Reyners AK, de Jong FA, Sparreboom A, van der Graaf WTA, Friberg LE, Schiavon G, Verweij J, Loos WJ, Mathijssen RHJ, de Giorgi U.
Correlations between imatinib plasma concentrations and clinical benefit in gastrointestinal stromal tumor (GIST) patients will be time point specific: results of a long-term prospective population pharmacokinetic study.
Submitted

IV. Fransson MN, Brugård J, Aronsson P, Gréen H.
Semi-physiologically based pharmacokinetic modelling of paclitaxel metabolism and in silico-based study of the dynamic sensitivities in pathway kinetics.
Submitted

CONTENTS

LIST OF ABBREVIATIONS

Biological and medical:

ABCB1	ATP-binding cassette, sub-family B (MDR/TAP), member 1
ADE	Adverse drug event
CYP2C8	Cytochrome P450, family 2, subfamily C, polypeptide 8
CYP3A4	Cytochrome P450, family 3, subfamily A, polypeptide 4
GIST	Gastrointestinal stromal tumor
OATP	Organic Anion-Transporting Polypeptides

Technical:

AIC	Akaike Information Criterion
AUC	Area Under Curve
FOCE	First-Order Conditional Estimation
IIV	Interindividual variability
LLP	Log-Likelihood Profiling
OFV	Objective Function Value
PK	Pharmacokinetics
PPK	Population pharmacokinetics
SE	Standard error
VPC	Visual Predictive Check

"A fanatic is one who can't change his mind and won't change the subject."

Winston Churchill

1 Introduction

Interindividual pharmacokinetic variability can be described as the variability in drug plasma concentrations among individuals in a population. Since plasma concentrations are easily accessible using a simple blood test, they are very important in order do understand the exposure of the drug on the body. For very potent drugs, such anticancer drugs, which often affect both healthy tissue and tumours, administrating a proper dose is crucial. Many anticancer drugs have a narrow *therapeutic window*, meaning that the difference is relatively small between an ineffective and a harmful dose. At the same time anticancer drugs often have a high pharmacokinetic variability, and plasma concentrations may vary 2-10-fold between patients [88].

The sources causing pharmacokinetic variability can be categorized as external factors related to medical care, lifestyle or environment, and internal factors related to individual biological characteristics. External factors may for instance comprise diet, patient compliance and drug interactions from co-medications, while internal factors include genetic differences in drug-transport and drug metabolizing systems, amount of body fat, age-related hepatic blood flow, or hepatic dysfunction caused by the disease [88].

1.1 Problem formulation

To minimize side effects from the treatment, *adverse drug events* (ADEs), the sources causing pharmacokinetic variability need to be understood. Some adverse drug events, such as hair loss and nausea, may be inevitable or can be handled using proper co-medication. More serious adverse events, like severe neurotoxicity or bone marrow suppression, may on the other hand make it necessary to interrupt the treatment.

Quantifying additional suffering from ADEs in individuals already carrying the burden of a serious disease is difficult. Even if patients must be kept in focus, the cost for society may be more easily estimated. A study in the United States by Hassett et al. [31] investigated the various costs with respect to chemotherapy given to women under age 64 suffering from breast cancer. It was estimated that only the chemotherapy-related serious ADEs themselves were on average $1 271 per person and year. It was also estimated that each year in the U.S. alone there are 35 000 women

under age 64 suffering from breast cancer that receive chemotherapy and therefore the total cost for these ADEs may reach $45 million per year. Stokes et al. [83] evaluated the specific costs related to neutropenia (i.e., decreased count of the most common type of white blood cell - neutrophils) in first-line chemotherapy treatment of non-small cell lung cancer in patients aged 65 years or older in the U.S. For the more serious form of neutropenia, afflicting almost 10% of the approximately 5 000 studied individuals, costs from ADEs were estimated to $2 700 per patient and month [83].

Also in treatment using targeted anticancer drugs, which in contrast to chemotherapeutic drugs are specifically aimed at the tumour cells, ADEs may be substantial as recently reported by Borovicka et al. [7]. They estimated adverse dermatologic toxicities in a small group of 130 patients to a median cost of $1 920 per patient.

Reported costs for ADEs may to some extent relate to different attitudes to prevention and different skill levels at the clinics [71], or may not be directly attributable to pharmacokinetic variability. However, because of the high additional costs for ADEs also minor progress in individualized drug therapy based on reduced pharmacokinetic variability could give significant savings, not to mention the prospect of fewer afflicted patients.

In this thesis, internal factors potentially causing pharmacokinetic variability in two anticancer drugs are investigated using modelling and analysis of mathematical models.

1.2 Outline

The rest of the thesis is organized in the following way: Chapters 2 and 3 give the medical and technical background to the work. Chapters 4 to 6 define the aims of the thesis, describes the mathematical methods, patient material and software used. In Chapter 7 the results from Papers I-IV are discussed, and Chapter 8 summarizes the findings.

Note about bold text: To help the reader, several of the chapters or sections start with a bold text section where the content of the section is summarized. These sections do not contain any references and have intentionally been written in a somewhat simplified language than what is otherwise used. It is the wish of the author that the content of this thesis is available to as large an audience as possible.

2 Medical background

2.1 Paclitaxel

***Paclitaxel* is a naturally occurring substance that is derived from the tree Pacific Yew. Together with the chemically closely related semi-synthetic substance *docetaxel* it make up the *taxane* group of anticancer drugs. Paclitaxel inhibit cell division by stiffening parts of the cell skeleton, and is used in cancer treatment (chemotherapy) primarily against ovarian, breast and non-small cell lung cancer. Like other chemotherapeutic drugs, paclitaxel do not specifically target tumour cells but may affect all cells, and have an effect against cancer because tumour cells divide more rapidly than normal cells.**

2.1.1 The drug

The discovery of paclitaxel was due to a major survey, initiated by the U.S. National Cancer Institute in the late 1950s, with the goal to identify naturally occurring anti-cancer substances. Bark extract from the Pacific Yew (*lat. Taxus brevifolia*) was found to have anti-tumour effect, and in 1971 paclitaxel was identified as the underlying cytotoxic substance [70]. The actual mechanism was identified in 1979 as stabilization of microtubules [74]. By binding to the protein β-tubulin, which together with α-tubulin composes the microtubules, paclitaxel will promote stabilization of the microtubules to a degree where they cannot disassemble at cell proliferation, with cell death as result [70].

Figure 2.1 describes the metabolism of paclitaxel, which itself is the active substance. Hepatic metabolism of paclitaxel is a one- or two-step process involving the cytochrome P450 enzyme family. Paclitaxel is first metabolized to the CYP2C8 product *6α-hydroxypaclitaxel* [67], the main metabolite [29, 50], or the CYP3A4/3A5 product *p-3'-hydroxypaclitaxel* [30]. 6α-hydroxypaclitaxel and p-3'-hydroxypaclitaxel can then be further metabolized to *6α-, p-3'-dihydroxypaclitaxel*, by CYP3A4/3A5 or CYP2C8, respectively [82]. *In vitro* studies have estimated that approximately 60% of the first step of the liver metabolism of paclitaxel is via CYP2C8 [13]. Both

paclitaxel and its three metabolites are mainly cleared via feces, with approximately 70% of the dose cleared by this route [91].

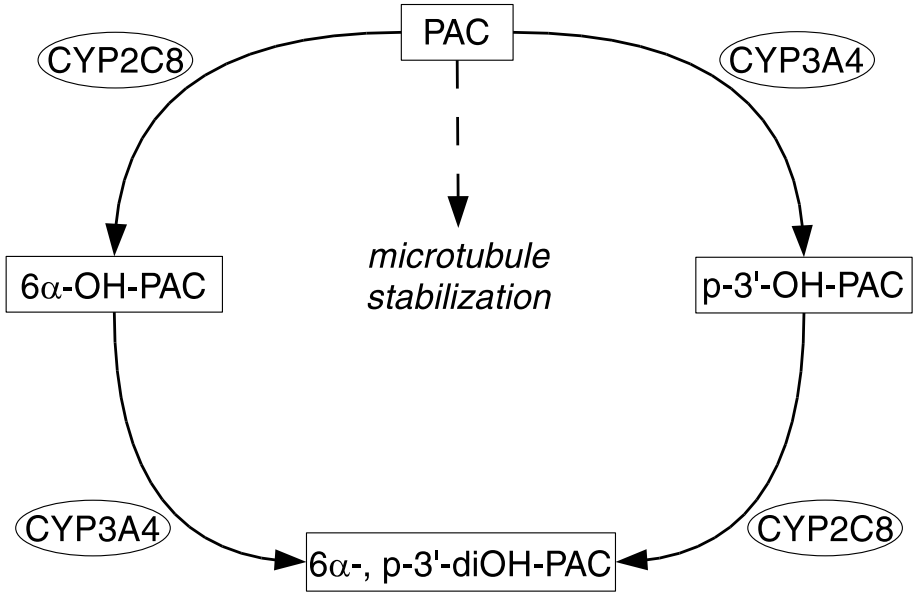

Figure 2.1: The metabolism of paclitaxel (PAC) in the liver to 6α-hydroxypaclitaxel (6α-OH-PAC), p-3'-hydroxypaclitaxel (p-3'-OH-PAC) and 6α-, p-3'-dihydroxypaclitaxel (6α-, p-3'-diOH-PAC). Squares represent substances and ellipses represent enzymes. The effect is shown with a dashed arrow.

In vitro experiments have demonstrated that hepatocellular uptake of paclitaxel is carried out by OATP1B3, a member of the membrane transport proteins known as organic anion-transporting polypeptides (OATP) [80], while cellular efflux is facilitated by ABCB1 (P-glycoprotein/P-gp, mdr-1), a member of the ATP-binding cassette [41].

Because paclitaxel plasma concentrations show a large interindividual variability, several studies have investigated associations between pheno- and genotypes and pharmacokinetics. Significant findings include gender, age, body weight, and bilirubin [36, 43]. The metabolizing enzymes and transport proteins described above have also been the subject of investigation in several studies, [6, 27, 37, 59, 79, 97]. The outcome of these studies are inconclusive; of the two largest studies Henningsson et al. [37] found no associations for polymorphisms in CYP2C8, CYP3A4, CYP3A5 or ABCB1, while Bergmann et al. [6] reported CYP2C8*3 to be associated with 11% lower clearance of paclitaxel.

2.1.2 Cremophor EL

Because of its poor solubility in water and biological fluids, such as plasma, paclitaxel is commonly administrated in an equal mixture of the nonionic solubilizer *Cremophor EL*® (BASF Corp.), a castor oil derivative, and ethanol [21]. The trademark for

this specific combination is *Taxol*® (Bristol-Myers Squibb). Although many adverse drug events from treatment with Taxol are attributable to paclitaxel, it has also been shown that ADEs like hypersensitivity reactions may be caused by Cremophor EL itself [21, 34]. Further, it has been shown that the solubilizer alters the pharmacokinetics of paclitaxel, since total plasma concentrations of paclitaxel typically follow nonlinear (saturable) pharmacokinetics [23, 81] while unbound plasma concentrations of paclitaxel follow linear pharmacokinetics [35, 36]. Notably, docetaxel, for which another solubilizer than Cremophor EL is used, has also been described using linear pharmacokinetics [8, 51].

2.1.3 Ovarian cancer

Ovarian cancer is a group of three different forms of cancer that all relate to the ovaries. The most common one is *epithelial ovarian cancer*, which is estimated to cover 90% of all cases of ovarian cancer, while stromal ovarian cancer and germ cell ovarian cancer each account approximately equally for the remaining cases [2]. According to global statistics from 2008, ovarian cancer is the seventh most common cancer-related death world-wide in the female population, with approximately 226 000 new cases annually, and 140 000 deaths [42]. It is estimated that 10% of all cases are due to factors of inheritance, and of these do 90% relate to mutations in two specific genes *BRCA1* and *BRCA2* [84], which are also related to breast cancer. Decreased risk is associated with, e.g., pregnancy, breastfeeding and the use of birth control pills [84].

Surgery is the most important method for diagnostics of ovarian cancer, and also the primary approach for treatment of the disease. If tumours are found, the stage of the disease is measured by the International Federation of Gynecology and Obstetrics (FIGO) staging system. The FIGO system consists of four main stages (I-IV), where stage I is the least serious, with tumour growth limited to the ovaries, and stage IV is the most serious, with distant metastases. Because 75% of cases are diagnosed at stage III or IV, diagnosis is often poor [63].

Postoperative treatment with chemotherapy is almost always recommended, with a few exceptions [2, 55]. The standard treatment comprise a three-hour intravenous infusion of paclitaxel 175 mg/m^2 in combination with carboplatin, given every third week for six cycles [84, 85]. If relapse occurs the patient may be re-treated using the same or other drugs depending on her development of drug resistance. Although paclitaxel is administrated in relation to the patients' body-surface area, differences in interindividual plasma concentrations are large. The risk for relapsing patients to develop drug resistance and the fact that paclitaxel may cause serious ADEs emphasizes the importance of individualized drug therapy.

2.2 Imatinib

***Imatinib* can be considered to be the first developed anticancer drug that was specifically designed to target certain kinds of tumour cells. By binding to and inhibiting a specific protein, it decreases the activity of tumour cells and causes cell death. Originally developed for treatment of a particular type of leukemia, imatinib is now also used in treatment of gastrointestinal stromal tumour and other cancers that expresses the specific protein.**

2.2.1 The drug

Imatinib (imatinib mesylate, Gleevec, Glivec), was developed during the 90s as an inhibitor for a specific type of *tyrosine kinase*, BCR-ABL, a fusion oncoprotein expressed in the malignant cells of chronic myeloid leukaemia [20]. Imatinib was also found to inhibit the KIT tyrosine kinase, for which mutations are frequent in gastrointestinal stromal tumours [10, 12].

Imatinib has a bioavailability of 98% [61] and is mainly metabolized in the liver by CYP3A4/3A5 to the active metabolite CGP 74588 [17]. The drug is mainly excreted in feces (67%) and to a smaller amount in urine (13%) [28].

2.2.2 Gastrointestinal stromal tumour

Gastrointestinal stromal tumour (GIST) is believed to origin from the interstitial cells of Cajal (ICC) [12], i.e., the cells that uses electrical signalling to stimulate the smooth muscles in the gastrointestinal tract, causing the contraction essential for processing of nutrients. An import characteristic and biomarker for GIST are specific mutations in the KIT tyrosine kinase receptor. KIT-mutations are present in about 85% of GISTs, while mutations in another tyrosine kinase receptor, the PDGFRA, is present in about 5% [10] of cases. KIT is important since normal tissue usually contains an equilibrium of non-active receptors and receptors activated by extracellular ligands [12]. In most GIST, the tyrosine kinase receptors are activated without the ligands, which results in further activation of signalling pathways and ultimately transcription of oncogenes [12].

GIST usually origins in the stomach or the small intestine; 60% of cases, or in the small intestine; 30% of cases [10]. Although distant metastasis occur, the tumour usually only metastasize to nearby tissue, such as the liver. Based on data between 1983 and 2000, Nilsson et al. [60] estimated the annual incidence of GIST in Sweden to 14.5 per million, while the prevalence was 129 per million for all GIST risk groups. Before the inclusion of imatinib in treatment of GIST, conventional chemotherapy

was used, usually with very poor response. Following the introduction of imatinib in treatment of advanced GIST, the median survival time has increased from 18 months to 5 years, where 34% of the patients survive more than 9 years [12].

The standard dosing scheme for imatinib in treatment of patients with advanced GIST or relapsed patients, consists of a 400 mg oral dose daily, often with treatment lasting at least one year [10]. Although the response rate to imatinib therapy is affected by the primary oncogenic mutation in the tyrosine kinase receptors, adherence is also important to keep disease control, and since secondary mutations often lead to drug resistance [3, 12].

"Nothing in life is to be feared,
it is only to be understood."

Marie Curie

3 Technical background

3.1 Model building of dynamical systems

The description of the distribution of a drug in the body or the elimination in the liver can often be approximated by a mathematical model, consisting of time-depending equations called *differential equations*. Specifically, the well-known *Michaelis-Menten equation* can be described in this setting. It is commonly used to describe a concentration-dependent or *saturated* process, for which an increase in drug concentration only will cause increased enzymatic drug elimination up to a certain concentration limit, after which the elimination will remain at the same rate.

3.1.1 Systems and models

Consider a system $\mathcal{S}$, represented by the cloud-like shape in Figure 3.1, for which the inner structure is more or less known. The understanding of the system can be improved by studying its behaviour, i.e., by making observations or performing measurements on parts of it. Such measurable information is called *output signals*. If these are dependent on time, $\mathcal{S}$ is called a *dynamical system* and the output signals will be denoted $\boldsymbol{y}(t)$ (from here on bold text indicates a vector or a possible vector). Apart from measuring the output signals, it may be possible to directly affect the system in a way such that its output signals changes. If this is the case the dynamical system is said to also have one or more *input signals*, denoted $\boldsymbol{u}(t)$. In this setting, the boundaries of the system can be described by its input and output signals.

The process of creating a model $\mathcal{M}$ of $\mathcal{S}$ can be performed in many ways. It will depend on a number of factors, for instance i) the prior knowledge about $\mathcal{S}$, ii) the possibilities to vary input signals, iii) the possibilities of measuring the output signals and iv) the choice of modelling tools. Creating a model based on these features is the subject of the area of *system identification*. For extensive reading see for instance Ljung [53].

A common way to represent a model mathematically is with ordinary differential

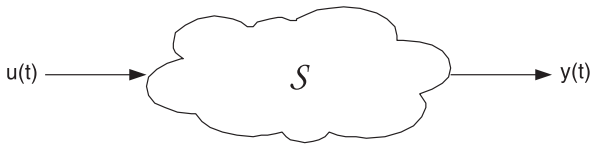

Figure 3.1: A dynamic system $\mathcal{S}$ with input $\boldsymbol{u}(t)$ and output $\boldsymbol{y}(t)$.

equations, which may be nonlinear. If the following formulation is used:

$$\dot{\boldsymbol{x}}(t) = \boldsymbol{f}(\boldsymbol{x}(t), \boldsymbol{u}(t), \boldsymbol{\theta}) \tag{3.1a}$$

$$\boldsymbol{y}(t) = \boldsymbol{h}(\boldsymbol{x}(t), \boldsymbol{u}(t), \boldsymbol{\theta}) \tag{3.1b}$$

the model is said to be on *state-space form*. In (3.1), $\boldsymbol{x}(t) = (x_1(t), \ldots, x_n(t))^T$ (a vector of n *state-variables*), $\dot{\boldsymbol{x}}(t) = (\dot{x}_1(t), \ldots, \dot{x}_n(t))^T$ (the vector of corresponding time derivatives), $\boldsymbol{u}(t) = (u_1(t), \ldots, u_m(t))^T$ (a vector of m input signals), $\boldsymbol{y}(t) = (y_1(t), \ldots, y_p(t))^T$ (a vector of p output signals), $\boldsymbol{\theta} = (\theta_1, \ldots, \theta_r)^T$ (a vector of r parameters) and $\boldsymbol{f}(\cdot) = (f_1(\cdot), \ldots, f_n(\cdot))^T$ and $\boldsymbol{h}(\cdot) = (h_1(\cdot), \ldots, h_p(\cdot))^T$ (vectors of the respective functions). Since observations often are discrete it is sometimes preferable to view the output signals as such as well. For this purpose a general model will, instead of (3.1), be denoted:

$$\dot{\boldsymbol{x}}(t) = \boldsymbol{f}(\boldsymbol{x}(t), \boldsymbol{u}(t), \boldsymbol{\theta}) \tag{3.2a}$$

$$\boldsymbol{y}_j = \boldsymbol{h}(\boldsymbol{x}_j, \boldsymbol{u}_j, \boldsymbol{\theta}) \tag{3.2b}$$

where $\boldsymbol{y}_j$ is the jth vector of output signals, measured at time t_j, and $\boldsymbol{x}_j = \boldsymbol{x}(t_j)$ and $\boldsymbol{u}_j = \boldsymbol{u}(t_j)$.

It is important to remember that any model of the system $\mathcal{S}$ is just a model. This means that it will most likely never be possible to explain the behaviour of the output information at all times, but perhaps only the main characteristics under certain conditions.

3.1.2 Mass-action and Michaelis-Menten kinetics

The following example is a modified version of the example found in Edelstein-Keshet [16]. Similar examples can also be found in most literature concerned with general biochemistry [5] or enzyme kinetics [77].

Consider a drug molecule, denoted X_1, in the body of a patient that is being treated for some medical condition. Although the objective of the drug dosage is to produce an improvement of the current condition of the patient, the drug is in most cases still a foreign substance from a bodily perspective. Fractions of the drug dose will therefore never reach its target within the body, but instead undergo detoxification

in some organ, most commonly in the liver. The detoxification process is handled by one or several classes of proteins acting as enzymes. Let the specific class of enzymes being responsible for the elimination of the drug be denoted by X_2. Assume that each enzyme handles exactly one drug molecule at a time. The process may then be described according to:

$$X_1 + X_2 \xrightarrow{k_1} X_3 \tag{3.3a}$$

$$X_1 + X_2 \xleftarrow{k_{-1}} X_3 \tag{3.3b}$$

$$X_3 \xrightarrow{k_2} X_4 + X_2 \tag{3.3c}$$

where the drug-enzyme complex is denoted by X_3, in (3.3a). The reaction can then either be reversed forming X_1 and X_2 in (3.3b), or proceed so that the parent drug molecule X_1 is converted to its metabolite X_4 that dissociate from the enzyme X_2 in (3.3c). k_1, k_{-1} and k_2 are the rate constants associated with the reactions in (3.3a)–(3.3c) respectively. Instead of working with the singular molecules X_1, X_2, X_3 and X_4 it may be preferable to work with the corresponding concentrations c_1, c_2, c_3 and c_4. For, e.g c_3, the law of mass action now implies that:

$$\text{Rate of formation of } c_3 = k_1 c_1 c_2 \tag{3.4a}$$

$$\text{Rate of break-down of } c_3 = -k_{-1} c_3 - k_2 c_3 \tag{3.4b}$$

Using mass action kinetics on all concentrations give the following system of differential equations:

$$\dot{c}_1(t) = -k_1 c_1(t) c_2(t) + k_{-1} c_3(t) \tag{3.5a}$$

$$\dot{c}_2(t) = -k_1 c_1(t) c_2(t) + k_{-1} c_3(t) + k_2 c_3(t) \tag{3.5b}$$

$$\dot{c}_3(t) = k_1 c_1(t) c_2(t) - k_{-1} c_3(t) - k_2 c_3(t) \tag{3.5c}$$

$$\dot{c}_4(t) = k_2 c_3(t) \tag{3.5d}$$

where $\dot{c}_i(t)$ denotes the time derivative of $c_i(t)$. Equations (3.5) are valid if it can be assumed that no new enzymes are formed during the time for which the chemical reactions are occurring. This implies that the time considered for the process should be sufficiently small, but how small depends on the specific system. Adding (3.5b) and (3.5c), gives:

$$\dot{c}_2(t) + \dot{c}_3(t) = 0 \tag{3.6}$$

and it becomes apparent that the concentration E_{tot} of all enzymes, both unoccupied and occupied, is constant during the process:

$$c_2(t) + c_3(t) = E_{tot} \Leftrightarrow c_2(t) = E_{tot} - c_3(t) \tag{3.7}$$

(3.5) can now be reduced by inserting (3.7) in (3.5a) and (3.5c). Also, since none of the equations in (3.5) depend on c_4, (3.5d) does not need to be considered, which gives:

$$\dot{c}_1(t) = -k_1 E_{tot} c_1(t) + (k_{-1} + k_1 c_1) c_3(t) \tag{3.8a}$$

$$\dot{c}_3(t) = k_1 E_{tot} c_1(t) - (k_{-1} + k_2 + k_1 c_1(t)) c_3(t) \tag{3.8b}$$

If no further assumptions regarding the system should be done, equations (3.8) will be the final model. However, reduction to a simpler model is possible with the *quasi-steady-state assumption*, which will provide the *Michaelis-Menten equation*.

A common property for enzymatic systems such as (3.8) is that the equilibrium of $c_3(t)$ is attained a lot faster than that of $c_1(t)$. Thus, under such specific circumstances it can be allowed to assume quasi-steady-state and set:

$$\dot{c}_3(t) \approx 0 \tag{3.9}$$

Then, solving (3.8b) for c_3 yields:

$$c_3(t) = \frac{k_1 E_{tot} c_1(t)}{k_{-1} + k_2 + k_1 c_1(t)} \tag{3.10}$$

This expression can be inserted into (3.8a), which then simplifies to:

$$\dot{c}_1(t) = -\frac{V_{max} c_1(t)}{K_M + c_1(t)} \tag{3.11}$$

where

$$V_{max} = k_2 E_{tot} \tag{3.12}$$

and

$$K_M = \frac{k_{-1} + k_2}{k_1} \tag{3.13}$$

(3.11) is the *Michaelis-Menten equation* and V_{max} is the maximal reaction rate that occurs when the concentration of occupied enzymes equals the total concentration of enzymes. K_M is usually called the *Michaelis constant*, and is equal to the drug concentration at which the reaction rate is half of V_{max}.

3.2 Pharmacokinetics

Pharmacokinetic modelling **basically means trying to build a model of what the body does with the drug. Mechanisms related to absorption, distribution and elimination of the drug are studied. This is in contrast to**

***pharmacodynamic modelling*, where the focus is what the drug does with the body, or simply the effect of the drug. Both types of modelling often includes the use of differential equations to describe drug concentrations or drug effects.**

3.2.1 Compartment models

Depending on the administration, distribution and elimination characteristics of a drug, measured plasma concentrations as function of time will give rise to different curvatures. To be able to model the decrease in drug concentration in plasma, the body is usually considered to consist of one or more compartments. Since they cannot in general be related to any kind of physiological compartments, these compartments should be considered to be empirical [33, 68].

If a drug is administrated as, e.g., an intravenous injection the absorption phase does not need to be considered. In that case, the number of compartments that are used to fit the measured concentrations will be equal to the degree of a multi-exponential function. If interpolation of measured plasma concentrations cause a plot like the one in Figure 3.2, a one compartment model with linear elimination may be sufficient to model the pharmacokinetics. The mathematical representation will then simply be a mono-exponential function:

$$c_p(t) = c_0 e^{-k_{10}t} \tag{3.14}$$

where c_0 is the initial drug concentration and k_{10} (also commonly denoted k_{el}) is the rate at which the drug is being eliminated. Graphically, this model can be represented by Figure 3.3.

Since the drug dose is given as a specific amount, and not as a concentration based on the distribution volume, it may be convenient to rewrite (3.14) on state-space form and symbolically also adding an input signal:

$$\dot{x}(t) = -k_{10}x(t) + u(t) \tag{3.15a}$$

$$c_p(t) = \frac{1}{V}x(t) \tag{3.15b}$$

where the state-variable $x(t)$ is the amount in mol and the input signal $u(t)$ is some function corresponding to the dose input. V is the apparent volume of the single compartment and can in this case be considered to be the same as the volume of distribution V_d.

Another example of a typical decrease of the drug concentration in plasma as a function of time is given in Figure 3.4. In this case taking the logarithm reveals that two compartments should be used in the pharmacokinetic model. The mathematical

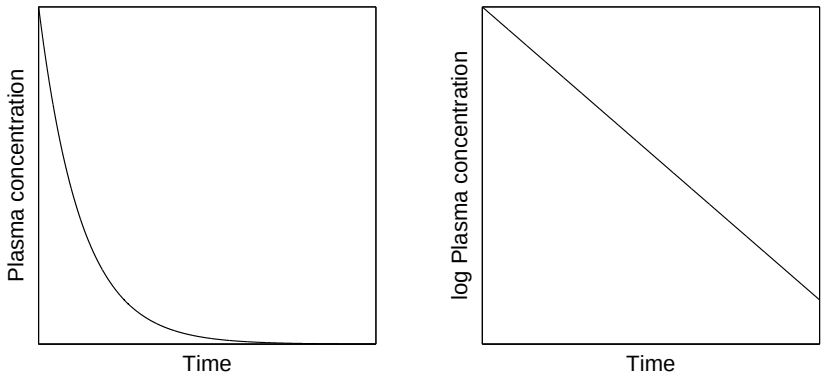

Figure 3.2: *Left:* The decrease in plasma concentration after a bolus dose. *Right:* By taking the logarithm of the plasma concentrations it becomes apparent that a one-compartment model may be used.

Figure 3.3: The graphical representation of (3.14).

model then becomes:

$$\dot{x}_1(t) = -(k_{10} + k_{12})x_1(t) + k_{21}x_2(t) + u(t) \tag{3.16a}$$

$$\dot{x}_2(t) = k_{12}x_1(t) - k_{21}x_2(t) \tag{3.16b}$$

$$c_p(t) = \frac{1}{V_1}x_1(t) \tag{3.16c}$$

where k_{12} and k_{21} are rate constants and V_1 is the apparent distribution volume of compartment one. Its corresponding graphical representation is seen in Figure 3.5. Instead of using rate constants (or *micro constants*) such as k_{10}, k_{12} and k_{21}, a parameter, Q, representing the intercompartmental volume flow, clearance CL, and apparent volumes V_1 and V_2, for each respective compartments may be preferred. Hence, using the reparameterization:

$$k_{10} = \frac{CL}{V_1},\ k_{12} = \frac{Q}{V_1},\ k_{21} = \frac{Q}{V_2} \tag{3.17}$$

(3.16) can be expressed as:

$$\dot{x}_1(t) = -\frac{CL}{V_1}x_1(t) - \frac{Q}{V_1}(x_1(t) - x_2(t)) + \frac{1}{V_1}u(t) \tag{3.18a}$$

$$\dot{x}_2(t) = \frac{Q}{V_2}(x_1(t) - x_2(t)) \tag{3.18b}$$

$$c_p(t) = \frac{1}{V_1}x_1(t) \tag{3.18c}$$

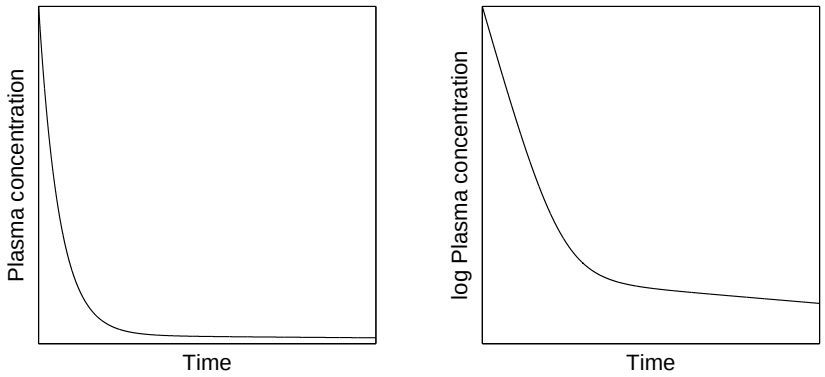

Figure 3.4: *Left:* A second example of a typical decrease in plasma concentration after a bolus dose. *Right:* Taking the logarithm of the plasma concentration reveals that a two-compartment model may be used.

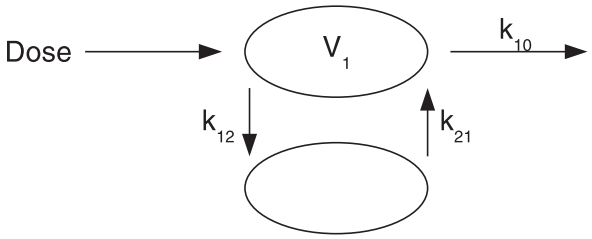

Figure 3.5: The graphical representation of (3.16).

Finally, an example is given in Figure 3.6 in the case when the drug elimination does not seem to be linear for logarithmic plasma concentrations. In the right plot it can be seen how the elimination appears to be slower during the initial period of time than at the end. This behaviour is typical for a capacity limited elimination process. In the beginning the system is saturated and elimination is independent of concentration. First after plasma concentrations have been reduced to a certain level will the elimination appear to be linear. By replacing $-k_{10}x(t)$ in (3.15a) with (3.11), an appropriate model for this process can be expressed as:

$$\dot{x}(t) = -\frac{V_{max}\frac{x(t)}{V}}{K_M + \frac{x(t)}{V}} + u(t) \tag{3.19a}$$

$$c_p(t) = \frac{1}{V}x(t) \tag{3.19b}$$

where the concentration $c(t)$ in (3.11) has been replaced by the amount $x(t)$ scaled by the volume V.

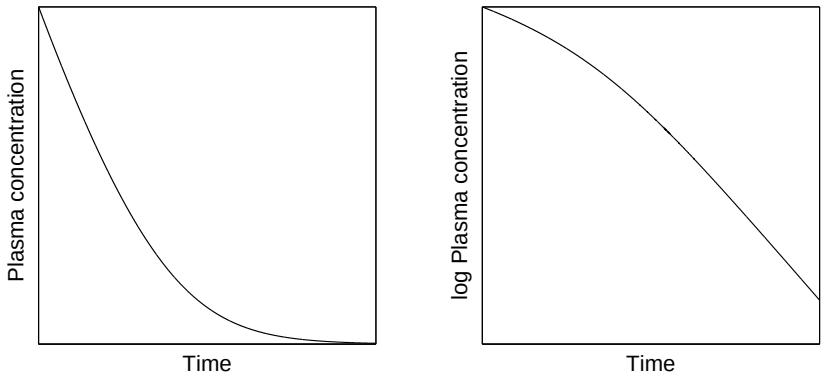

Figure 3.6: *Left:* A third example of a typical decrease in plasma concentration after a bolus dose. *Right:* The logarithmic plot indicates a saturated elimination process.

3.2.2 Population pharmacokinetics

Clinical studies may often be categorized according to *sparse* or *rich* sampling. Sparse data sets consist of only a few observations per individual, while rich data sets consist of perhaps eight or more observations; however, there does not seem to be any strict definitions. Also when working with a rich data set, building a specific model one at a time based only on the observations for one individual will in many cases not be practical. In the case of model (3.18) there are four parameters to estimate. With perhaps only ten observations, there may be many sets of parameter estimates that will fit the data.

The issue can be handled in the model building procedure by considering that data from all individuals will be used simultaneously. By assuming a common model structure for all individuals, and letting some or all parameters belong to a statistical distribution, parameters can be estimated from the complete data set. This approach is called *population pharmacokinetics* (PPK) and use the framework of *nonlinear mixed effects modelling* [4]. In general, this can be seen as an extension of (3.2):

$$\dot{\boldsymbol{x}}_i(t) = \boldsymbol{f}(\boldsymbol{x}_i(t), \boldsymbol{u}_i(t), \boldsymbol{\phi}_i) \tag{3.20a}$$

$$\boldsymbol{y}_{ij} = \boldsymbol{h}(\boldsymbol{x}_{ij}, \boldsymbol{u}_{ij}, \boldsymbol{\phi}_i) + \boldsymbol{\varepsilon}_{ij} \tag{3.20b}$$

$$\boldsymbol{\phi}_i = \boldsymbol{g}(\boldsymbol{z}_i, \boldsymbol{\theta}) + \boldsymbol{\eta}_i \tag{3.20c}$$

where each individual i will have its own *structural model*; (3.20a) and (3.20b), and where the subscript j refers to the jth observation for that individual. $\boldsymbol{\phi}_i$ is the vector of individual specific parameter values and $\boldsymbol{\varepsilon}_{ij}$ is the residual error (or *intraindividual variability*), which is assumed to belong to a normal distribution with mean zero and covariance matrix $\boldsymbol{\Sigma}$. The relation between $\boldsymbol{\phi}_i$ and the vector of typical parameter values for the population, $\boldsymbol{\theta}$, and the vector of covariates, $\boldsymbol{z}_i$, is governed by $\boldsymbol{g}(\cdot)$ in the *parameter model* (3.20c). Differences between $\boldsymbol{\phi}_i$ and $\boldsymbol{g}(\cdot)$ that cannot be explained by

any covariates, will be accounted for by the *interindividual variability* (IIV) term $\boldsymbol{\eta}_i$, which is assumed to belong to a normal distribution with zero mean and covariance matrix $\boldsymbol{\Omega}$. Both the residual error, $\boldsymbol{\varepsilon}_{ij}$, and the IIV, $\boldsymbol{\eta}_i$, can enter the model in different ways, such as additively as in (3.20), proportionally or exponentially.

Extending the model (3.18) to a PPK model could mean using an IIV exponentially on the parameter CL, while also assuming a proportional residual error:

$$\dot{x}_{1,i}(t) = -\frac{CLe^{\eta_i}}{V_1}x_{1,i}(t) - \frac{Q}{V_1}(x_{1,i}(t) - x_{2,i}(t)) + \frac{1}{V_1}u_i(t) \tag{3.21a}$$

$$\dot{x}_{2,i}(t) = \frac{Q}{V_2}(x_{1,i}(t) - x_{2,i}(t)) \tag{3.21b}$$

$$c_{p,ij} = \frac{1}{V_1}x_{1,ij}(1 + \varepsilon_{ij}) \tag{3.21c}$$

In addition to the residual error and the IIV, other forms of variability can also be included, such as *interoccasion variability* (IOV), which is important to consider in the case of having multiple study occasions from the same individual in the data set [48]. A further extension of (3.20) to stochastic differential equations has also been made, [86, 87], where the approach is to separate the residual error to measurement error and system noise using the extended Kalman filter [46, 87].

3.3 Identifiability

When estimating model parameters from data it may be a good idea to investigate the *identifiability* of the model, meaning if it is possible to obtain unique solutions for the parameter estimates. The identifiability concept can be separated into *structural identifiability*, which relates only to the model structure, independently of data, and *practical identifiability*, which relates to combination of the model structure and the data set.

3.3.1 Structural identifiability

Structural identifiability can be understood by considering a modified version of the one-compartment model (3.15). Assume that (3.15) is fitted to plasma concentrations for a specific drug. However, also assume that it is known that the drug elimination process is governed by two independent elimination mechanisms, A and B, each with its own corresponding rate constant. Hence it would be desirable to incorporate this knowledge into the model. Graphically this can be viewed as an alteration of Figure 3.2 to Figure 3.7. By also expressing the model mathematically as:

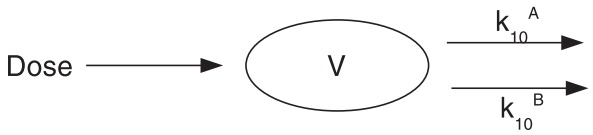

Figure 3.7: A one compartment model with two separate elimination mechanisms A and B, and their respective rate constants k_{10}^A and k_{10}^B.

$$\dot{x}(t) = -(k_{10}^A + k_{10}^B)x(t) + u(t) \tag{3.22a}$$

$$c_p(t) = \frac{1}{V}x(t) \tag{3.22b}$$

it becomes apparent that the two rate constants in the current model setting are indistinguishable. Only the sum $k_{10}^A + k_{10}^B$ can be estimated, regardless if the output signal $c_p(t)$ is considered to be "perfect", i.e., a continuous signal without any noise. Thus, for this kind of identifiability problem it is the structure of the model rather than the data that causes the problem. For the case of (3.22) one will simply have to be satisfied with estimating the sum of the two parameters, at least unless some kind of prior knowledge can be incorporated in another way, e.g., an approximate value of either k_{10}^A or k_{10}^B is known.

In this work a model is considered to be *globally* structural identifiable if a unique solution to the estimation problem exists without any restrictions on the parameter space, and *locally* structurally identifiable if a unique solution to the estimation problem exists, at least within a small region of the parameter space. For instance, the model:

$$\dot{x}(t) = -(k_{10})^2 x(t) + u(t) \tag{3.23a}$$

$$c_p(t) = \frac{1}{V}x(t) \tag{3.23b}$$

is not identifiable without any restrictions on k_{10}, since only $(k_{10})^2$ can be estimated uniquely, which could mean both $-k_{10}$ and k_{10} are valid solutions. But if only positive estimates $k_{10} > 0$ are considered the parameter, and hence the model, will be identifiable. The model is locally structural identifiable since a unique solution exists if the parameter space is restricted to all positive real numbers.

Further, the output signal is considered to be continuous, noise free and it is also assumed that no excitation problems of the system exist or any numerical problems during the estimation process [11]. Moreover, the identifiability properties of a model are only valid for a specific state-space form, since reparameterization or removal of output signals may change the structural identifiability. For a more formal definition of identifiability see, e.g., Ljung [53].

3.3.2 Practical identifiability

Even if a model is proved to be structural identifiable the data to which the model is to be fitted may be too sparse to get reliable estimates. In this case the model is overparameterized for the data at hand. Another problem could be if the data does not excite the model in the right way. Assume for instance that prior knowledge suggests the use of a one-compartment model with saturated elimination such as (3.19) for concentrations of a specific drug measured in plasma. However, if the current study uses a much lower drug dosage with the outcome that:

$$c_p(t) = \frac{1}{V}x(t) << K_M \tag{3.24}$$

the model (3.19) will during the estimation process behave approximately as:

$$\dot{x}(t) \approx -\frac{V_{max}}{K_M}\frac{x(t)}{V} + u(t) \tag{3.25a}$$

$$c_p(t) = \frac{1}{V}x(t) \tag{3.25b}$$

From this perspective V_{max} and K_M will be indistinguishable and large variances will most likely accompany the parameter estimates, if the minimization is at all successful. This is an example of practical (non-)identifiability. The simplest solution to the problem would be to use a one-compartment model with linear elimination such as (3.15), in which case the rate constant k_{10} will correspond to the quota of V_{max} and K_M, divided by V. Similar examples as the one presented and how to handle these are discussed by Cedersund [11].

4 Aims

The overall aim of the thesis is to explore the possibilities for individualized treatment of two specific anticancer drugs, by developing models to investigate their pharmacokinetic variability.

Specific aims

- To compare two pharmacokinetic models for paclitaxel and investigate if the mechanistically more plausible model can be used even if limitations in data will cause identifiability problems.
- To investigate the influence of the drug solubilzer Cremophor EL on paclitaxel metabolite kinetics and to investigate correlations of clearance of paclitaxel and its metabolites with enzyme activity and genetic polymorphisms.
- To develop a population pharmacokinetic model for imatinib and to investigate correlations between pharmacokinetics and liver metastasis.
- To develop a semi-physiologically based pharmacokinetic model describing the uptake, metabolism and efflux of paclitaxel and its metabolites and investigate the effect of potential genetic polymorphisms.

5 Methods

Several different methods may be used during model building, which is often a loop-like process including parameter estimation from data, testing identifiability and sensitivity of model parameters, and validating model performance.

5.1 Nonlinear mixed effects models - Papers I, II & III

Parameter estimation of the population pharmacokinetic models presented in Section 3.2.2 is conducted by the framework of nonlinear mixed effects models. Because it is assumed that any variability entering the model has its origin from a known distribution, in particular a normal distribution, likelihood-based methods can be used for estimation. It is also assumed that each individual i has its own statistical model, which is based on all the observation data $\boldsymbol{y}_i = (y_{i1}, \ldots, y_{iM})^T$ for that individual. Each model can be said to be parameterized by an individual specific vector $\boldsymbol{\eta}_i$, which is an instance of a normal distribution with mean zero and covariance matrix $\boldsymbol{\Omega}$ (the IIV, see Section 3.2.2), by the vector $\boldsymbol{\theta}$ of population median values, and of the residual covariance matrix $\boldsymbol{\Sigma}$. The goal is hence to estimate $\boldsymbol{\theta}$, $\boldsymbol{\Sigma}$ and $\boldsymbol{\Omega}$ from all data sets $\boldsymbol{y}_i$, $i = 1, \ldots, N$, where N is the number of individuals. For individual i the probability of the data set $\boldsymbol{y}_i$ given $\boldsymbol{\theta}$, $\boldsymbol{\Sigma}$ and $\boldsymbol{\Omega}$ will thus be $P(\boldsymbol{y}_i|\boldsymbol{\theta}, \boldsymbol{\Sigma}, \boldsymbol{\Omega})$, or $L_i(\boldsymbol{\theta}, \boldsymbol{\Sigma}, \boldsymbol{\Omega}|\boldsymbol{y}_i)$, which is the individual contribution to the population likelihood L. Considering the expressions to be marginal distributions over $\boldsymbol{\eta}_i$, gives:

$$\begin{aligned} P(\boldsymbol{y}_i|\boldsymbol{\theta}, \boldsymbol{\Sigma}, \boldsymbol{\Omega}) = L_i(\boldsymbol{\theta}, \boldsymbol{\Sigma}, \boldsymbol{\Omega}|\boldsymbol{y}_i) &= \int P(\boldsymbol{y}_i, \boldsymbol{\eta}_i|\boldsymbol{\theta}, \boldsymbol{\Sigma}, \boldsymbol{\Omega}) d\boldsymbol{\eta}_i \\ &= \int P(\boldsymbol{y}_i|\boldsymbol{\eta}_i, \boldsymbol{\theta}, \boldsymbol{\Sigma}, \boldsymbol{\Omega}) P(\boldsymbol{\eta}_i|\boldsymbol{\theta}, \boldsymbol{\Sigma}, \boldsymbol{\Omega}) d\boldsymbol{\eta}_i \\ &= \int P(\boldsymbol{y}_i|\boldsymbol{\eta}_i, \boldsymbol{\theta}, \boldsymbol{\Sigma}) P(\boldsymbol{\eta}_i|\boldsymbol{\Omega}) d\boldsymbol{\eta}_i \\ &= \int l_i(\boldsymbol{\eta}_i, \boldsymbol{\theta}, \boldsymbol{\Sigma}|\boldsymbol{y}_i) p_\eta(\boldsymbol{\eta}_i|\boldsymbol{\Omega}) d\boldsymbol{\eta}_i \end{aligned} \tag{5.1}$$

where $l_i(\boldsymbol{\eta}_i, \boldsymbol{\theta}, \boldsymbol{\Sigma}|\boldsymbol{y}_i)$ is the individual likelihood function associated with the structural model (3.20a)-(3.20b), and $p_\eta(\boldsymbol{\eta}_i|\boldsymbol{\Omega})$ is the density function associated with the

parameter model (3.20c). The second equality from the end in (5.1) follows from $\boldsymbol{y}_i$ not being explicitly dependent on $\boldsymbol{\Omega}$ if $\boldsymbol{\eta}_i$ is given, and $\boldsymbol{\eta}_i$ not being dependent on $\boldsymbol{\theta}$ or $\boldsymbol{\Sigma}$. Further, the population likelihood L for the complete data set $\mathcal{Y}$ is given by:

$$L(\boldsymbol{\theta}, \boldsymbol{\Sigma}, \boldsymbol{\Omega}|\mathcal{Y}) = \prod_{i=1}^{N} L_i(\boldsymbol{\theta}, \boldsymbol{\Sigma}, \boldsymbol{\Omega}|\boldsymbol{y}_i) \tag{5.2}$$

and taking $-2\log$ of (5.2) gives:

$$\begin{aligned} -2\log L(\boldsymbol{\theta}, \boldsymbol{\Sigma}, \boldsymbol{\Omega}|\mathcal{Y}) &= \sum_{i=1}^{N} \left[-2\log L_i(\boldsymbol{\theta}, \boldsymbol{\Sigma}, \boldsymbol{\Omega}|\boldsymbol{y}_i)\right] \\ &= \sum_{i=1}^{N} \left[-2\log \int l_i(\boldsymbol{\eta}_i, \boldsymbol{\theta}, \boldsymbol{\Sigma}|\boldsymbol{y}_i) p_\eta(\boldsymbol{\eta}_i|\boldsymbol{\Omega}) d\boldsymbol{\eta}_i\right] \end{aligned} \tag{5.3}$$

5.1.1 First-Order Conditional Estimation in NONMEM

Because the integral in (5.3) is difficult to calculate exactly, different approximations are often used. In NONMEM (Materials chapter, Section 6.2.1) several methods are available that approximates (5.3); let:

$$\Phi_i(\boldsymbol{\eta}_i) = -2\log l_i(\boldsymbol{\eta}_i, \boldsymbol{\theta}, \boldsymbol{\Sigma}|\boldsymbol{y}_i) \tag{5.4}$$

and denote its gradient vector $\nabla_{\Phi_i}(\boldsymbol{\eta}_i)$, and the hessian matrix $\Delta_{\Phi_i}(\boldsymbol{\eta}_i)$. If Laplace's method for approximation of integrals is used it can then be shown that an approximation for $-2\log L_i(\boldsymbol{\theta}, \boldsymbol{\Sigma}, \boldsymbol{\Omega}|\boldsymbol{y}_i)$ in (5.3) is given by:

$$\begin{aligned} &\hat{\Phi}_i + \log|\boldsymbol{\Omega}| + \hat{\boldsymbol{\eta}}_i^T \boldsymbol{\Omega}^{-1} \hat{\boldsymbol{\eta}}_i + \log\left|\boldsymbol{\Omega}^{-1} + \frac{1}{2}\hat{\Delta}_{\Phi_i}\right| \\ &- \left(\frac{1}{2}\hat{\nabla}_{\Phi_i} + \boldsymbol{\Omega}^{-1}\hat{\boldsymbol{\eta}}_i\right)^T \left(\boldsymbol{\Omega}^{-1} + \frac{1}{2}\hat{\Delta}_{\Phi_i}\right)^{-1} \left(\frac{1}{2}\hat{\nabla}_{\Phi_i} + \boldsymbol{\Omega}^{-1}\hat{\boldsymbol{\eta}}_i\right) \end{aligned} \tag{5.5}$$

where $\hat{\boldsymbol{\eta}}_i$ is some estimate of $\boldsymbol{\eta}_i$, and $\hat{\Phi}_i$, $\hat{\nabla}_{\Phi_i}$ and $\hat{\Delta}_{\Phi_i}$ are the respective functions evaluated at $\hat{\boldsymbol{\eta}}_i$ [4]. If $\hat{\boldsymbol{\eta}}_i$ is the mode obtained by maximizing the joint likelihood $l_i(\boldsymbol{\eta}_i, \boldsymbol{\theta}, \boldsymbol{\Sigma}|\boldsymbol{y}_i) p_\eta(\boldsymbol{\eta}_i|\boldsymbol{\Omega}) d\boldsymbol{\eta}_i$, over $\boldsymbol{\eta}_i$, the last term in (5.5) will vanish (compare with the first-order derivative of a function optimum). Further, the Hessian, $\Delta_{\Phi_i}(\boldsymbol{\eta}_i)$, can be approximated by using first-order derivatives:

$$\Delta_{\Phi_i}(\boldsymbol{\eta}_i) \approx \frac{1}{2} E\left(\nabla_{\Phi_i}(\boldsymbol{\eta}_i) \nabla_{\Phi_i}(\boldsymbol{\eta}_i)^T\right) \tag{5.6}$$

where E is the expectation over $\boldsymbol{y}_i$ for each individual structural model (3.20a)-(3.20b) [92]. Inserting (5.6) in (5.5), while omitting the last term, gives:

$$\hat{\Phi}_i + \log|\boldsymbol{\Omega}| + \hat{\boldsymbol{\eta}}_i^T \boldsymbol{\Omega}^{-1} \hat{\boldsymbol{\eta}}_i + \log \left| \boldsymbol{\Omega}^{-1} + \frac{1}{4} E\left(\nabla_{\Phi_i}(\boldsymbol{\eta}_i) \nabla_{\Phi_i}(\boldsymbol{\eta}_i)^T \right) \right|_{\hat{\boldsymbol{\eta}}_i} \tag{5.7}$$

where the bracket subscript, $|_{\hat{\boldsymbol{\eta}}_i}$, denotes that $\hat{\boldsymbol{\eta}}_i$ will be inserted after the expectation over $\boldsymbol{y}_i$ has been evaluated. The NONMEM method described in (5.7) is the *First-Order Conditional Estimation* (FOCE) method, and can in turn be approximated in several ways. For more information about the methods in NONMEM see the NONMEM User's Guides [4] and the derivations by Wang [92].

5.1.2 Objective Function Value and Akaike Information Criterion

Similar to the other estimation methods in NONMEM, the FOCE is used to calculate the *Objective Function Value* (OFV), which is hence proportional to $-2 \times$ log likelihood of the data. For two nested models, the OFV can be used directly for model comparison because a difference in OFV, ΔOFV, is approximatively χ^2-distributed and can hence be used to perform a likelihood ratio test [4]. For instance, an additional parameter resulting in $\Delta\text{OFV} < -3.84$ will thus be significant for $p < 0.05$.

For non-nested models, the OFV can still be used in model comparison by applying the Akaike Information Criterion (AIC). AIC is expressed as:

$$\text{AIC} = \text{OFV} + 2h \tag{5.8}$$

where h is the number of all parameters, both θs, ω^2s and σ^2s, that are estimated by NONMEM, while fixed parameters are not considered. Similar to ΔOFV, the difference in AIC between two models, ΔAIC, can then be used to select the best model. A rough rule of thumb has been suggested by Burnham and Anderson [9], where the level of empirical support for an alternative model is suggested to be "substantial" for $\Delta\text{AIC} = [0, 2]$, "considerably less" for $\Delta\text{AIC} = [4, 7]$, and "essentially none" for $\Delta\text{AIC} > 10$. For the theory and derivation of the AIC, see for instance Ljung [53].

5.2 Local algebraic observability test - Paper I

Investigating structural identifiability can be seen as a special case of the more general *observability* problem, which is concerned with determining whether a state-variable is observable from input and output signals. By considering a parameter θ to be a state-variable for which $\dot{\theta} = 0$, structural identifiability can be investigated using the framework of observability. A measure of the complete dynamics of a model given on

state-space form (3.1) with a single output y, n state-variables and r parameters can be described by the matrix O:

$$O = \begin{pmatrix} \frac{\partial y}{\partial x_1} & \cdots & \frac{\partial y}{\partial x_n} & \frac{\partial y}{\partial \theta_1} & \cdots & \frac{\partial y}{\partial \theta_r} \\ \frac{\partial \dot{y}}{\partial x_1} & \cdots & \frac{\partial \dot{y}}{\partial x_n} & \frac{\partial \dot{y}}{\partial \theta_1} & \cdots & \frac{\partial \dot{y}}{\partial \theta_r} \\ \vdots & & \vdots & \vdots & & \vdots \\ \frac{\partial y^{(n+r)}}{\partial x_1} & \cdots & \frac{\partial y^{(n+r)}}{\partial x_n} & \frac{\partial y^{(n+r)}}{\partial \theta_1} & \cdots & \frac{\partial y^{(n+r)}}{\partial \theta_r} \end{pmatrix} \tag{5.9}$$

If the matrix is of full rank $n + r$ the model is structural identifiable [76]. If however the rank test reveals that some columns are linearly dependent the model suffers from overparameterization. To determine which parameters that are non-identifiable, one column can be removed at a time and the effect on the rank of O can be checked. No change indicates that the particular column removed corresponds to a non-identifiable parameter. The number of columns that has to be removed for O to obtain full rank is called its *transcendence degree*, and an identifiable model will thus have a transcendence degree of zero [11, 76].

The symbolic derivations of the functions used in the matrix elements in (5.9) can rapidly become quite cumbersome and acquire much computational time depending on the size of the model. Sedoglavic [76] has presented an algorithm that bypasses this problem by instead of calculating exact expressions uses Taylor approximations. By using this approach and some other techniques the computations can be made in polynomial time, i.e., the number of steps required to solve the algorithm will be polynomial with respect to the complexity. It is a probabilistic algorithm in the aspect that only if the model is observable the answer is for certain correct, while there is a small possibility of an incorrect answer in the case of a non-observable model. However, the probability of a correct answer in this case is very high. An example presented by Sedoglavic [76], which comprises a model where the number of state-variables $n = 4$ and the number of parameters $r = 17$, is shown to be non-observable with a probability of 0.9993.

5.3 Frequentist priors - Paper II

For population pharmacokinetic models a special kind of method for handling identifiability problems has been developed. It relies on the use of prior information in the form of estimates of parameters and variances from earlier developed models. The information is incorporated into the current model so as to mimic the resemblance if

the data from the earlier study was also available. This approach will thus stabilize any estimates with respect to such *informative priors* [22] or *frequentist priors* [24].

Reserving the use of OFV to numerical values, and instead denote the NONMEM objective function OF, the terminology in Section 5.1 can be used to express the OF as:

$$\text{OF} \propto -2\log L = \sum_{i=1}^{N} [-2\log L_i] \tag{5.10}$$

Further, let OF_i denote the individual contributions to the objective function OF, so that:

$$\text{OF} = \sum_{i=1}^{N} \text{OF}_i \tag{5.11}$$

where the individual contributions could be summarized partially, making up two contributions, e.g., OF_A and OF_B:

$$\text{OF} = \sum_{i=1}^{k} \text{OF}_i + \sum_{i=k+1}^{N} \text{OF}_i = \text{OF}_A + \text{OF}_B \tag{5.12}$$

In essence, the OF will be defined by the data set $\mathcal{Y}$, and the model structure under consideration, $\mathcal{M}$. Hence, the OF can be regarded as a function, $\text{OF}(\mathcal{Y}, \mathcal{M})$. The total OF can then be described as:

$$\text{OF}(\mathcal{Y}, \mathcal{M}) = \text{OF}_A(\mathcal{Y}_{1,k}, \mathcal{M}) + \text{OF}_B(\mathcal{Y}_{k+1,N}, \mathcal{M}) \tag{5.13}$$

Now assume that only the data for the first k individuals, $\mathcal{Y}_{1,k}$, are available for model building. Also assume that the data for the remaining individuals, $\mathcal{Y}_{k+1,N}$, have been used previously to estimate parameters for the model structure $\mathcal{M}$, and that the model $\mathcal{M}(\mathcal{Y}_{k+1,N})$ is available, including parameter estimates and standard errors. Although the data set $\mathcal{Y}_{k+1,N}$ is not directly available, its representation in terms of the model $\mathcal{M}(\mathcal{Y}_{k+1,N})$ is. To describe the total OF, the aim will thus be to find a function OF^P so that:

$$\text{OF}^P(\mathcal{M}(\mathcal{Y}_{k+1,N})) \approx \text{OF}_B(\mathcal{Y}_{k+1,N}, \mathcal{M}) \tag{5.14}$$

If the vectors of geometric means $\boldsymbol{\theta} = (\theta_1, \theta_2, ...)$ (i.e., the typical population values) and geometric variances $\boldsymbol{\omega^2} = ((\omega_1)^2, (\omega_2)^2, ...)$ (i.e., the interindividual variability) estimated from $\mathcal{M}(\mathcal{Y}_{k+1,N})$ can be considered independent, the joint density function of a normal distribution and inverse-Wishart distribution, with ν degrees of freedom, can be used as the function OF^P. This is the *Normal-inverse Wishart Prior*, described by Gisleskog et al. [24], where the *Normal* corresponds to the multivariate normal distribution of $\boldsymbol{\theta}$, and the *inverse-Wishart* corresponds to the distribution of the di-

agonal matrix $\boldsymbol{\Omega}$ comprising the elements of $\boldsymbol{\omega^2}$. OF^P will work as a penalty function, since the sum $\mathrm{OF}_A + \mathrm{OF}^P$ will be at minimum if the new estimates based on the data set $\mathcal{Y}_{1,k}$ and the previous estimates, $\boldsymbol{\theta}$ and $\boldsymbol{\omega^2}$, resemble each other. In NONMEM, the required information for this approach are the priors of $\boldsymbol{\theta}$ and $\boldsymbol{\omega^2}$, including their standard errors. The number of degrees of freedom ν for each ω^2, may then be derived from the respective standard error SE_{ω^2} of the variance ω^2:

$$SE_{\omega^2} = \omega^2 \cdot \sqrt{\frac{2}{\nu - 1}} \Rightarrow \nu = \frac{2 \cdot \left(\omega^2\right)^2}{\left(SE_{\omega^2}\right)^2} + 1 \tag{5.15}$$

6 Materials

6.1 Patient material

Two different studies were used in the thesis work, the first one included thirty-three women receiving paclitaxel treatment for ovarian cancer, and the second one included fifty patients receiving imatinib treatment for gastrointestinal stromal tumour. The two studies differ in a number of ways; in the paclitaxel study only one series of measurements were performed for each patient, while the patients in the imatinib study had about three series of measurements each, with several months apart. In the paclitaxel study patients received their medication from a three-hour infusion, and in the imatinib study each patient should themselves take his or her medication each day for more than a year.

6.1.1 Paclitaxel study - Papers I & II

The main objective of the paclitaxel study was to investigate the role of the genetic polymorphisms in the metabolizing enzymes CYP2C8 and CYP3A4, and the membrane transport protein ABCB1 (P-gp, mdr-1) in the pharmacokinetics of paclitaxel. The study comprised thirty-three women, aged 36 to 75 years (median 62), with different types of gynaecological cancers: epithelial ovarian cancer ($n = 26$), peritoneal cancer ($n = 4$), ovarian or peritoneal ($n = 1$), carcinoma in corpus uteri ($n = 1$) and in cervix uteri ($n = 1$) as described by Green et al. [27]. The subjects received an intravenous infusion of paclitaxel (Taxol) for three hours, at 175 mg/m^2 ($n = 30$) or 135 mg/m^2 ($n = 3$, due to poor general condition) and carboplatin. Thirty-one subjects received at least six cycles of chemotherapy. One subject received only one cycle due to septicaemia and another subject was withdrawn after four cycles due to neurotoxicity.

Blood samples for pharmacokinetic analysis were collected during one cycle per subject, between the first and eighth cycle (median cycle number 3), and collected in EDTA tubes. The target times for sampling were; immediately before start of infusion, at 30 min and 1 h after start, immediately before stop of infusion, at 5,

15, 30 min and 1, 2, 4, 8 and 24 h after stop. Total concentrations of paclitaxel, 6α-hydroxypaclitaxel and p-3'-hydroxypaclitaxel were analyzed in samples from all subjects, while 6α-, p-3'-dihydroxypaclitaxel, was analyzed in samples from fifteen subjects. Samples were analyzed using solid phase extraction, reverse-phase high-performance liquid chromatography and an ion trap mass spectrometer with a sonic spray ionization interphase as described by Green et al. [26]. The number of samples used in data analysis is presented in Table 6.1.

Enzyme activity for CYP3A4 *in vivo* could be determined in thirty-one subjects by quinine administration prior to start of chemotherapy, as described by Mirghani et al. [57, 58]. Genetic polymorphisms in CYP2C8, CYP3A4 and ABCB1 were determined in all subjects using Pyrosequencing according to the protocol of the manufacturer and as previously described [25, 27].

Table 6.1: Pharmacokinetic (PK) data for the paclitaxel study ($n = 33$)

PK samples	Considered	Missing (BQL[b])	Excluded[c]	Used
Paclitaxel	352	2 (0)	5	345
6α-hydroxypaclitaxel	352	16 (12)	4	332
p-3'-hydroxypaclitaxel	352	13 (9)	3	336
6α-, p-3'-dihydroxypaclitaxel[a]	164	18 (6)	3	143
Total	1220	49 (27)	15	1156

[a]Fifteen subjects contributed with 6α-, p-3'-dihydroxypaclitaxel samples
[b]Some of the missing samples were possibly below quantification limit (BQL)
[c]Removed because of a large ($> 30\%$) within-sample variability in one subject

6.1.2 Imatinib study - Paper III

The objectives of the imatinib study were to develop a population pharmacokinetic model based on long-term imatinib treatment, and to investigate correlations between pharmacokinetics and liver metastasis. Fifty subjects (29 males, 21 females) diagnosed with gastrointestinal stromal tumour (GIST) were included in the study at the start of treatment, in two Dutch and two Italian medical centers. Patients already receiving drugs known to interact with the primary metabolizing enzyme(s) CYP3A4/3A5 were not included in the study, if no alternative medication was available.

Blood samples for pharmacokinetic analysis (rich occasions) were collected on the first day (Day 1) of imatinib treatment and mainly after 1, 6 and 12 months, see Table 6.2. During the rich occasions, blood samples were collected immediately before imatinib administration and 30 minutes, 1, 2, 3, 4, 6 and 24 hours after dose intake. In addition, on day 14, and monthly during the treatment, trough samples were taken immediately before the daily dose intake. Methods for blood sampling, storage, and sample analysis were conducted as previously described by Schiavon et al. [73].

Table 6.2: Number of rich occasions for each group of months for all fifty subjects

Months	Day 1	1[a], 2 and 3	5 and 6[b]	11[c], 12[c], 13, 14, 17, 18 and 22	Total
Occasions	50	49	45	45	189

[a] Month 1 contained 46 rich occasions
[b] Month 6 contained 40 rich occasions
[c] Months 11 and 12 contained together 37 rich occasions

Twenty-six subjects (13 males, 13 females) had liver metastasis. The volumes of liver metastasis and liver were assessed by Computed tomography (CT), at start of treatment, and after 6 and 12 months. Subjects not having liver metastasis were assigned a liver metastasis volume equal to zero, and hence also had a metastasis/liver volume ratio of zero. Imatinib observations lacking information on volume of liver metastasis and metastasis/liver volume ratio that belonged to subjects with metastasis were excluded, leaving 1363 imatinib observations (the covariate data set) of the 1743 observations (the full data set) that were eligible for data analysis. The number of samples used in data analysis is presented in Table 6.3.

Table 6.3: Pharmacokinetic (PK) data for the imatinib study ($n = 50$)

PK samples	Considered	Missing[a]	Excluded[b]	Used
Full data set	1820	10	67	1743
Covariate data set				1363

[a]Below quantification limit or assay error
[b]Time for sampling and/or the time for the preceding dose could not be determined

6.2 Software tools

Four main tools were used in the thesis work; NONMEM, which is a computer program for statistical analysis, was used to analyze the data from the paclitaxel and imatinib studies, and to build population pharmacokinetic models, MathModelica was used for model building that was not directly based on data from the studies, and Mathematica and Maple were used for further analysis of the models.

6.2.1 NONMEM - Papers I, II & III

NONMEM® (Icon Development Solutions) is a program written in Fortran and can be considered the gold standard software for nonlinear mixed effects modelling in population pharmacokinetics/-dynamics. Although developed for implementation and parameter estimation of models that are typically fitted to data from clinical studies involving several individuals, NONMEM can also be used as a general nonlinear regression tool. It uses a subroutine called *PRED* (prediction) to obtain predicted

values from regression analysis, and a specific subroutine called *PREDPP* (PRED for population pharmacokinetics) can be used to estimate parameters in population pharmacokinetic models. Several different estimation methods are available, where the ones used for parameter estimation in population pharmacokinetic models often uses likelihood-based estimation, see the Methods chapter, Section 5.1, and the NONMEM User's Guides [4].

NONMEM VI was used in Papers I and II, while NONMEM 7 was used in Paper III. For additional analyses and visualization of NONMEM results, the *Xpose* package for the statistical programming language *R*, was used [44, 66]. For automatization of NONMEM runs, Log-Likelihood Profiling (LLP), stepwise covariate modelling and bootstrap analysis, *Perl-speaks-NONMEM* (PsN) was used [52].

6.2.2 MathModelica - Papers I & IV

MathModelica® (MathCore Engineering AB) is a platform for the *Modelica* programming language, which is developed for object-oriented modelling and simulation of most dynamical systems (time-continuous, time-discrete or hybrid systems). The combination of an object-oriented approach and an equation-based language offers the possibility to create submodels of parts of a larger system and then connect these to a complete model. Another feature is that the information flow between components can be chosen to be either causal, i.e., the flow has a specified direction, or acausal, in which case the flow has no specific direction. In addition to the Modelica language, there is also an open-source Modelica Standard Library with predefined models, as well as a number of additional open-source or commercial libraries [18, 19].

The MathModelica software includes an editor for graphical and textual representation of models, *System Designer*, and a simulation environment, *Simulation Center* for performing model simulation experiments. Models and results from MathModelica can be imported to Mathematica, enabling further analysis using Mathematica functions.

MathModelica Professional 1.1 was used in combination with Mathematica 5.2 in Paper I for the AUC-based sensitivity analysis.

MathModelica Professional 3.0 was used in combination with Mathematica 8 in Paper IV for model building, constrained optimization and dynamic sensitivity analysis.

6.2.3 Mathematica - Papers I & IV

Mathematica® (Wolfram Research, Inc.) is a general purpose system and computer algebra system. Mainly, it uses a functional programming language, a property that for instance implies very concise representations of functions. [32, 95, 98].

Mathematica 5.2 was used in Paper I, were the function `NIntegrate` was used in the sensitivity analysis to check variations of the area under curve (AUC) for simulated plasma concentration.

Mathematica 8 was used in Paper IV, were the functions `NDSolve` and `FindMinimum` were used for the constrained optimization problem.

6.2.4 Maple - Paper I

Maple® (Maplesoft, Cybernet Systems Co., Ltd.) is a computer algebra system that mainly uses a procedural programming language [32, 54].

Maple 10 was used for the structural identifiability analysis of the pharmacokinetic models in Paper I. The analysis utilized a special package called `observabilityTest`, see Methods chapter, Section 5.2, and Sedoglavic [76]. From a user perspective, `observabilityTest` takes a model on state-space form as input and gives the transcendence degree and the set of non-observable state-variables and parameters as output.

"All we have to decide is what to do with the time that is given to us."

Gandalf Grey, *Lord of the Rings* by J.R.R. Tolkien

7 Results and Discussion

7.1 Paper I

Paper I aimed at comparing two published pharmacokinetic model structures for paclitaxel; the first one, denoted $\mathcal{M}_E$ (E for empirical), originally based only on total paclitaxel concentrations, and a more mechanism-based model structure, $\mathcal{M}_M$, originally based on both total and unbound paclitaxel concentrations, and also concentrations of the solubilizer Cremophor EL. Specifically, the aim was to investigate if the more mechanistic model structure, $\mathcal{M}_M$, could be used even if only total paclitaxel concentrations were available. Results showed that $\mathcal{M}_M$ had at least as good fit as $\mathcal{M}_E$, if identifiability issues were properly handled. This means that total concentrations can be used in combination with $\mathcal{M}_M$ to predict unbound concentrations, which are more relevant when investigating pharmacokinetic variability.

7.1.1 Identifiablity analysis

Use of the local algebraic observability test (Methods chapter, Section 5.2) indicated four parameters to be structurally non-identifiable for a reparametrized version of $\mathcal{M}_M$:

$$\mathcal{D} = \{V_{u1}, B_{CrEL}, B_{lin}, K_{MB}\} \tag{7.1}$$

where V_{u1} is the volume of distribution of the central compartment, B_{CrEL} is the binding directly proportional to the Cremophor EL plasma concentration, B_{lin} is the linear binding to plasma components and K_{MB} the unbound plasma concentration at half of the maximum binding to plasma (B_{max}).

In relation to the local algebraic observability test, it should be pointed out that the approach assumes that the Cremophor EL plasma concentration, $c_{CrEL}(t)$, is an additional input signal acting directly on the output of $\mathcal{M}_M$, i.e., the total paclitaxel concentration $c_{Mp}(t)$. However, in the differential algebraic setting [69] used in Sedoglavic [76] it is assumed that all inputs and their derivatives are independent. In reality, clearly $c_{CrEL}(t)$ is dependent on the paclitaxel dosage, $D_{pac}(t)$, because

Cremophor EL is the solubilizer for paclitaxel. Therefore the Cremophor EL dose is:

$$D_{CrEL}(t) = D_{pac}(t)/S \tag{7.2}$$

where S is a scaling parameter with the dimension ml/μmol, since $D_{CrEL}(t)$ has the dimension ml/h and $D_{pac}(t)$ is in μmol/h. Because the observability test tests algebraic dependence, two cases representative for this dependence were tried. The first case tested the observability for a completely independent input signal with respect to $D_{pac}(t)$ acting on $c_{Mp}(t)$. The second case tested a fully dependent signal with respect to $D_{pac}(t)$, i.e., $c_{CrEL}(t) = D_{pac}(t)$. Because the two cases provided the same set of non-identifiable parameters it was assumed that the degree of dependence between $c_{CrEL}(t)$ and $D_{pac}(t)$ was of less importance. The issue of input-output dependence should also be seen in relation to other potentially problematic assumptions necessary to use the observability test, such as the derivative of a step-like input signal, or system noise [11].

7.1.2 Sensitivity analysis and parameter fixing

Sensitivity analysis based on the change in AUC over 48 hours identified K_{MB} in (7.1) to be least sensitive. Because preliminary runs in NONMEM indicated problems with identifiability even after fixing K_{MB}, it was assumed additional parameters had to be fixed. Repeated NONMEM runs proved that fixing the parameters associated with the second peripheral compartment, Q_{u3} and V_{u3}, resulted in a stable model. The selection of these particular parameters was based on the comparison of estimates associated with the two peripheral compartments from two previous studies as reported by Henningsson et al. [35, 37], and presented in Table 7.1. Because V_{u2} is the

Table 7.1: Estimates reported by Henningsson et al. [35, 37] for parameters associated with the peripheral compartments

θ_M	Henningsson et al. [35]	Henningsson et al. [37]
Q_{u2} (l/h)	134	132
V_{u2} (l)	856	3450
Q_{u3} (l/h)	213	151
V_{u3} (l)	303	303

parameter that varies most between the two studies, the parameters of the second peripheral compartment, Q_{u3} and V_{u3} were fixed according to previous estimates [35]. Fixing the two parameters only resulted in an increase of +2.6 in the NONMEM OFV, which is non-significant for $p < 0.05$.

An additional sensitivity analysis for parameters Q_{u2}, V_{u2}, Q_{u3} and V_{u3} showed a small effect in general on the AUC over 48 hours, compared to the structurally

non-identifiable parameters in (7.1). The results are presented in Table 7.2. Fixing Q_{u3} and V_{u3} instead of, e.g., Q_{u2} and V_{u3}, will correspond to entirely fixing the rate-constant $K_{31} = Q_{u3}/V_{u3}$ in a reparametrized model.

Table 7.2: Estimates and deviations from Henningsson et al. [35] for intercompartmental clearances, Q_{u2}, Q_{u3}, volumes of distribution, V_{u2}, V_{u3}, and the structurally non-identifiable parameters in (7.1), with the change in AUC over 48 hours

θ_M	$\hat{\theta}_M^H$	$\hat{\theta}_M^{H,-2SE}$	$\hat{\theta}_M^{H,+2SE}$	$\delta^{H,-2SE}$ (%)	$\delta^{H,+2SE}$ (%)
Q_{u2} (l/h)	134	75	190	-0.27	0.13
V_{u2} (l)	856	600	1100	0.37	-0.63
Q_{u3} (l/h)	213	120	310	-0.8	0.59
V_{u3} (l)	303	180	430	0.24	-0.41
V_{u1} (l)	229	150	310	-1.2	1.0
B_{CrEL}	3.78	3.0	4.5	-12	11
B_{lin}	7.59	5.8	9.4	-7.9	8.0
K_{MB} (μmol/h)	0.000106	0.000015	0.00020	0.32	-0.24

7.1.3 Model comparison

Because the model structures $\mathcal{M}_E$ and $\mathcal{M}_M$ are not nested, the final models $\mathcal{M}_E(\hat{\theta}_E)$ and $\mathcal{M}_M(\hat{\theta}_M)$, was compared using the AIC, rather than the NONMEM OFV. The AIC favoured the fit of the mechanism-based model, $\mathcal{M}_M(\hat{\theta}_M)$, with $\Delta\text{AIC} = -31$. According to the rule of thumb (Methods chapter, Section 5.1.2), the difference may be considered large enough to fully omit the empirical model. However, because only variance elements were used in the $\mathbf{\Omega}$-matrices describing IIV, which is also the case in the studies by Henningsson et al. [35] and Joerger et al. [43], and covariances between random effects were not extensively studied, a more careful conclusion is preferred, stating that the model structure $\mathcal{M}_M$ is at least as good as and $\mathcal{M}_E$. This conclusion is also supported by the hold-out validation, which did not favour any of the two models.

7.2 Paper II

The purpose of Paper II was to develop a pharmacokinetic model for paclitaxel and its metabolites, using data from a clinical study consisting of thirty-three women on treatment for ovarian cancer. In particular, the influence of the drug solubilizer Cremophor EL, and genetic mutations (polymorphisms) in enzymes and transporter proteins on paclitaxel and metabolites were investigated. Similar to paclitaxel, the concentration curves of two of the metabolites were found to be influenced by the concentration of Cremophor EL. A small association was also found between the elimination of the main metabolite and one of the transporter proteins.

7.2.1 Model for paclitaxel metabolites

The final model structure for unbound concentrations, predicted from observed total concentrations, used a three-compartment model for paclitaxel, and one compartment each for the three metabolites, according to Figure 7.1. Because only total concentrations of paclitaxel and metabolites were available, frequentist priors (Methods chapter, Section 5.3) from the study by Henningsson et al. [35] were used to stabilize parameter estimation. The relation between total concentration $[\text{pac}]_\text{t}$ and unbound concentration $[\text{pac}]_\text{u}$ of paclitaxel, and concentration of Cremophor EL [CrEL] were described according to the model developed by Henningsson et al. [35]:

$$[\text{pac}]_\text{t} = [\text{pac}]_\text{u} + B_\text{lin} \cdot [\text{pac}]_\text{u} + B_\text{CrEL} \cdot [\text{CrEL}] \cdot [\text{pac}]_\text{u} + \frac{B_\text{max} \cdot [\text{pac}]_\text{u}}{K_\text{m} + [\text{pac}]_\text{u}} \tag{7.3}$$

The model in (7.3) can be compared to the corresponding relations between total and unbound concentrations of the hydroxy-metabolites 6α-hydroxypaclitaxel, [6αOH], and p-3'-hydroxypaclitaxel, [p3OH], developed in this paper:

$$[6\alpha\text{OH}]_\text{t} = [6\alpha\text{OH}]_\text{u} + \frac{B_{6\alpha\text{OH}} \cdot [\text{CrEL}]^{\text{Hill}_\text{CrEL}}}{(\text{CrEL}_{50})^{\text{Hill}_\text{CrEL}} + [\text{CrEL}]^{\text{Hill}_\text{CrEL}}} \cdot [6\alpha\text{OH}]_\text{u} + B_{\text{nsp},6\alpha\text{OH}} \cdot [\text{CrEL}] \tag{7.4a}$$

$$[\text{p3OH}]_\text{t} = [\text{p3OH}]_\text{u} + \frac{B_\text{p3OH} \cdot [\text{CrEL}]^{\text{Hill}_\text{CrEL}}}{(\text{CrEL}_{50})^{\text{Hill}_\text{CrEL}} + [\text{CrEL}]^{\text{Hill}_\text{CrEL}}} \cdot [\text{p3OH}]_\text{u} + B_\text{nsp,p3OH} \cdot [\text{CrEL}] \tag{7.4b}$$

where the Hill coefficient, Hill_CrEL, and CrEL_{50} are the same for the two metabolites. CrEL_{50} is the Cremophor EL concentration at half of the maximal binding rates, $B_{6\alpha\text{OH}}$, and B_p3OH, of the respective hydroxy-metabolites to potential Cremophor EL micelles. Interindividual variability (IIV) was used for B_lin, in (7.3), and for the Hill

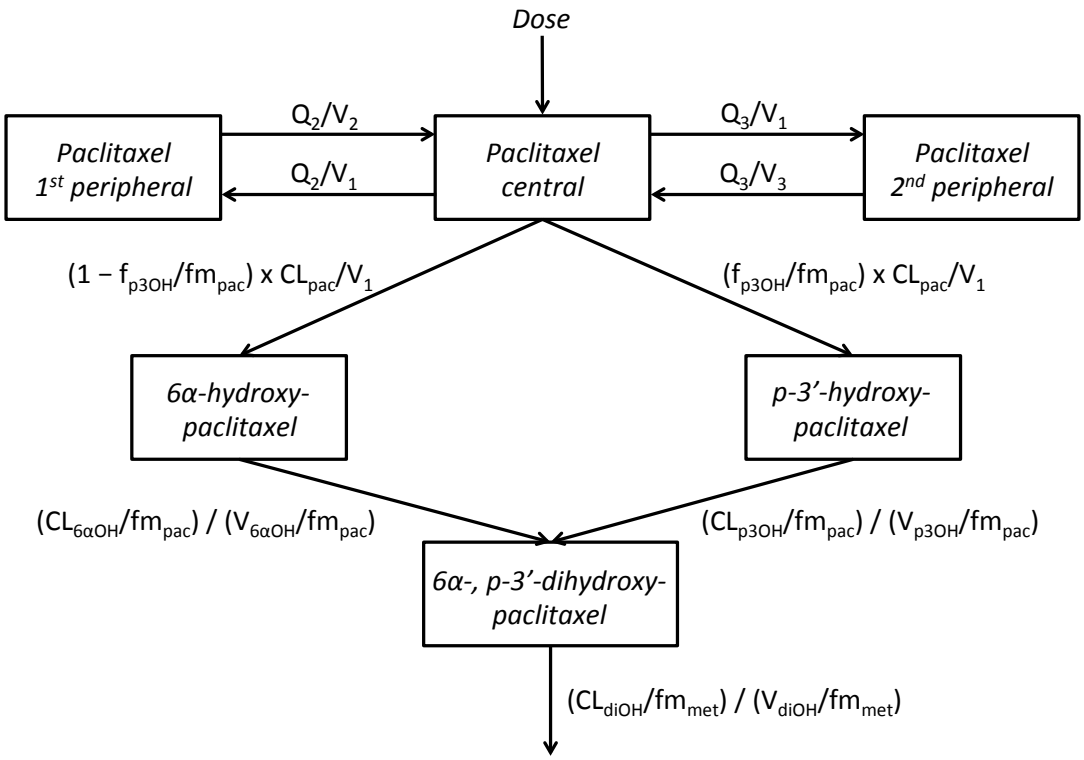

Figure 7.1: The compartment model for unbound concentrations.

coefficient, $\text{Hill}_{\text{CrEL}}$ in (7.4). Of the two previous population pharmacokinetic models based on both total and unbound paclitaxel concentrations, the first one by Henningsson et al. [35], from which the prior information used in this paper was acquired, did not use any IIV in binding parameters. In the second model, Henningsson et al. [36] used IIV in B_{CrEL} in (7.3), but the reported coefficient of variation (CV) was only 14%, which can be compared to the CV of 101% for IIV in the parameter describing plasma protein binding, B_{lin}, in this work. Since the present model was only based on total concentrations, used priors from a more heterogenous study [35], and used simulated Cremophor EL concentrations from another population pharmacokinetic model [38], it is likely that the large CV for IIV in B_{lin}, is partly caused by differences in models and data. This may also be the case for the relatively large CV of 41% for IIV in $\text{Hill}_{\text{CrEL}}$.

The Hill equation has earlier been proposed by Piszkiewicz [64, 65] as a model for micelle-catalyzed reactions, which give some support of its use as a binding model in this work. The Hill coefficient in (7.4), $\text{Hill}_{\text{CrEL}}$, was estimated to 2.71, which is in accordance with the range from approximately 1 to 6 of previously derived coefficients, for a number of combinations of detergents and substrates, as reported by Piszkiewicz [65]. The non-specific term in (7.4) was clearly significant for both

hydroxy-metabolites and seemed to be related to the Cremophor EL concentration. However, it should be pointed out that the non-specific term is empirical in nature, since it will make total metabolite concentrations depend explicitly on the concentration of the solubilizer. The significance of different elements in the binding model for hydoroxy-metabolites, as part of the final population pharmacokinetic model, is presented in Table 7.3.

Table 7.3: Significance of the different elements in the binding model for hydroxy-metabolites (7.4), as part of the final population pharmacokinetic model for paclitaxel and its three metabolites

Change	ΔOFV[a]	Δd.f.[b]
$\text{Hill}_{\text{CrEL}}$ fixed to 1 with no IIV	173	-2
No non-specific term (nsp) for $[\text{p3OH}]_t$ in (7.4b)	215	-1
No non-specific term (nsp) for $[6\alpha\text{OH}]_t$ in (7.4a)	114	-1
No IIV on $\text{Hill}_{\text{CrEL}}$	53	-1
No [CrEL] binding to non-specific terms (nsp)	21	0
Final model	0	0
Different CrEL_{50} for $[6\alpha\text{OH}]_t$ and $[\text{p3OH}]_t$	-2	1
Different $\text{Hill}_{\text{CrEL}}$ for $[6\alpha\text{OH}]_t$ and $[\text{p3OH}]_t$	-19	2

$[6\alpha\text{OH}]_t$, total concentration 6α-hydroxypaclitaxel; $[\text{p3OH}]_t$, total concentration p-3'-hydroxypaclitaxel; [CrEL], concentration Cremophor EL

[a] ΔOFV is relative to the final model

[b] Δd.f. is the difference in number of degrees of freedom

7.2.2 Covariate analysis

Stepwise covariate modelling was performed for genes ABCB1 (C3435T, G2677T/A), CYP2C8 (*1B, *1C, *3, *4), CYP3A4 (*1B) and CYP3A5 (*3) in all clearance parameters (CL). None of the tested associations were significant for $p < 0.01$. All associations found to be significant for $p < 0.1$, corresponding to a drop in OFV with at least 2.71 units for one additional degree of freedom, were subject to further investigation using two alternative models. In addition to parameters already included in the final model, both alternative models included IIV in V_1 and V_2, since these random effects where part of the model developed by Henningsson et al. [35], from which priors were adopted. In Alternative model 2, IIV in B_{lin} was excluded to exactly mimic the parametrization in the original model [35]. In addition to the log-likelihood ratio test using NONMEM OFV, an additional one-way ANOVA was performed using individual predicted estimates (empirical Bayes estimates) from the FOCE. The influence of the GM2677T/A variant on clearance of 6α-hydroxypaclitaxel, $\text{CL}_{6\alpha\text{OH}}/\text{fm}_{\text{pac}}$, was the only consistent association over all models and $p < 0.1$. For the final model, individuals carrying the polymorphisms G/A ($n = 3$) or G/G ($n = 5$) showed a 30% increase while individuals with polymorphism T/T ($n = 8$) showed a 27% decrease

relative the polymorphism G/T ($n = 17$). The effect estimates of G2677T/A were however accompanied with a high uncertainty, and the 95% and 90% CIs (but not the 80% CI) for the estimates included zero.

Since the current association has not been previously described, an additional analysis was carried out for the final and alternative models, only using paclitaxel concentrations. The purpose was to investigate whether the significant association was transmitted to clearance of paclitaxel, CL_{pac}, if no metabolite data was used. Results are presented in Table 7.4. In the absence of metabolite data, the GM2677T/A variant turned out to be significantly associated to paclitaxel clearance over all models for $p < 0.1$. This association is also apparent for alternative model 1, but not for the final model, when including metabolite data. It should be pointed out that IIV in distribution volumes never turned out to be significant parameters during the model building procedure, hence alternative model 1 was not used in the continued development. This particular model also showed identifiability issues in some cases, resulting in unreasonable high estimates. Overall, Table 7.4 may serve as an indication to why associations may sometimes be significant and sometimes not. The conclusion would be that several different combinations of data sets, models and significance tests may stand a better chance of eliciting these kind of weak associations, than a single model would.

Table 7.4: Covariate testing of the ABCB1 variant GM2677T/A for three different models, fitted to paclitaxel concentrations only, or both paclitaxel and metabolite concentrations

Model and parameter	ΔOFV[c]	p (ΔOFV)[d]	p (ANOVA)[e]
Model building based on paclitaxel concentrations only			
Final model			
CL_{pac}	5.65	0.059	0.024
Alternative model 1[a]			
CL_{pac}	8.86	0.012	0.0071
Alternative model 2[b]			
CL_{pac}	7.14	0.028	0.010
Model building based on paclitaxel and metabolite concentrations			
Final model			
CL_{pac}	2.23	0.33	0.21
$CL_{6\alpha OH}/fm_{pac}$	7.38	0.025	0.012
Alternative model 1[a]			
CL_{pac}	5.14	0.077	0.033
$CL_{6\alpha OH}/fm_{pac}$	4.79	0.091	0.048
Alternative model 2[b]			
CL_{pac}	3.42	0.18	0.073
$CL_{6\alpha OH}/fm_{pac}$	5.86	0.054	0.033

[a] Alternative model 1 = Final model with IIV_{V_1} and IIV_{V_2}
[b] Alternative model 2 = Alternative model 1 without $IIV_{B_{lin}}$
[c] For a model with fixed estimates instead of priors for paclitaxel parameters
[d] p-value based on the difference in OFV according to $\chi^2(2)$
[e] p-value based on one-way ANOVA of individual predicted estimates

7.3 Paper III

The primary aim of Paper III was to develop a pharmacokinetic model for imatinib, using data from a clinical study including fifty men and women on long-term treatment for gastrointestinal stromal tumour. Specifically, the model was intended to account for the possibility of decreasing plasma concentrations over time. As a secondary aim, the effect of liver metastasis on imatinib pharmacokinetics was investigated. Imatinib plasma concentrations were best fitted to a model that included a time delay between drug intake and absorption. In addition, it was found that the model should include mechanisms describing a substantial decrease in both the amount of drug that is absorbed and the rate of this absorption. A small effect was also found between the size of liver metastasis and drug clearance.

7.3.1 Population pharmacokinetic model

Because the data set contained both rich sample occasions and in-between trough samples, all dose events and observations in each individual data set were handled in a time-consecutive manner, from start to end of study, instead of using an approach comprising interoccassion variability [48]. Steady-state levels were obtained by assuming that dosing had occurred in 24-hour intervals for at least 10 days before a trough sample. Since imatinib was administrated orally, and no intravenous drug administration data was available, the bioavailability (F) was set to 1, meaning that clearance (CL) and volume of distribution (V) should be interpreted as the apparent clearance (CL/F) and volume of distribution (V/F), respectively. Observed plasma concentrations were log-transformed and residual errors were modelled using an additive error. Interindividual variability (IIV) was modelled exponentially.

Plasma concentrations of imatinib were best fitted to a two compartment model, with five transit compartments preceding the absorption compartment, according to Figure 7.2. The transit compartments were included in a step-wise manner during model development. The flexible way of determining an optimal non-integer number for transit compartments by use of the Sterling approximation, as described by Savic et al. [72], and adapted to handle multiple-dosing by Wilkins et al. [94], was considered but not implemented, since preliminary runs indicated that relatively few transit compartments could be used.

Previous population pharmacokinetic models for imatinib has mostly comprised one-compartment models, with zero-order [15, 45, 56, 75] or first-order [62, 89, 93] absorption and linear elimination. Previous studies using the population pharmacokinetic approach have in general used fewer imatinib observations ($\sim$ 100 to 800) with

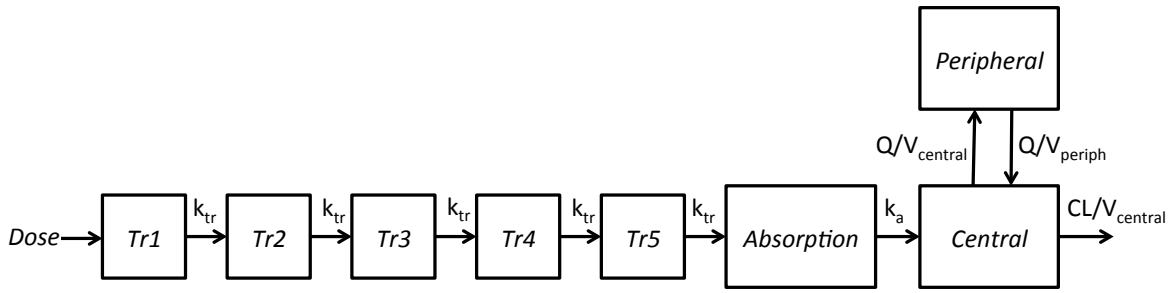

Figure 7.2: The population pharmacokinetic model for imatinib, with five transit compartments preceding the absorption, central and peripheral compartments.

fewer rich occasions and about the same number of subjects ($\sim$ 10 to 70), than the present study, which could account for its more elaborate model. Only the Phase III trial study of imatinib in treatment of chronic myeloid leukaemia by Schmidli et al. [75], surpasses in total number of observations ($m = 1930$) and number of subjects ($n = 371$), although this study had considerably less samples per subject due to a different sampling schedule with a shorter study period.

7.3.2 Time dependency

Adding time dependency on the bioavailability F and the absorption k_a largely decreased the OFV compared to a model without time dependency, as can be seen in Table 7.5, by comparing models no 1 and 7. Figure 7.3 describes the time dependence in F and k_a. Notably, the time dependency in F, could be replaced by an almost equally good fit with a time dependent CL (Table 7.5, models no 6 and 7), resulting in an increasing clearance with time, but this model was not robust and highly sensitive to initial estimates. At least two previous studies using population pharmacokinetic modelling have found evidence of time dependent imatinib pharmacokinetics; the Phase III trial study by Schmidli et al. [75] reported a decreased CL from 14 to 10 l/h from Day 1 to Day 29, while Judson et al. [45] reported an increase in CL with 33% after 12 months of treatment, which is in accordance with the current study. Petain et al. [62] reported a decreased clearance (over the fraction metbolized) for the metabolite CGP 74588, but not for imatinib, after 30 days compared to start of treatment.

The importance of including time dependency in F and k_a can be further visualized by comparison of Visual Predictive Checks (VPC) [40]. The VPC in Figure 7.4 is based on the final model with time dependency in F and k_a, but without any covariates. This model has been fitted to all the rich occasions over all months and also trough samples for subjects with no metastasis. On the other hand, the VPC in Figure 7.5 is based on a model where the time dependency in F and k_a has been removed, and the model has been fitted only to the first sampling occasion in the

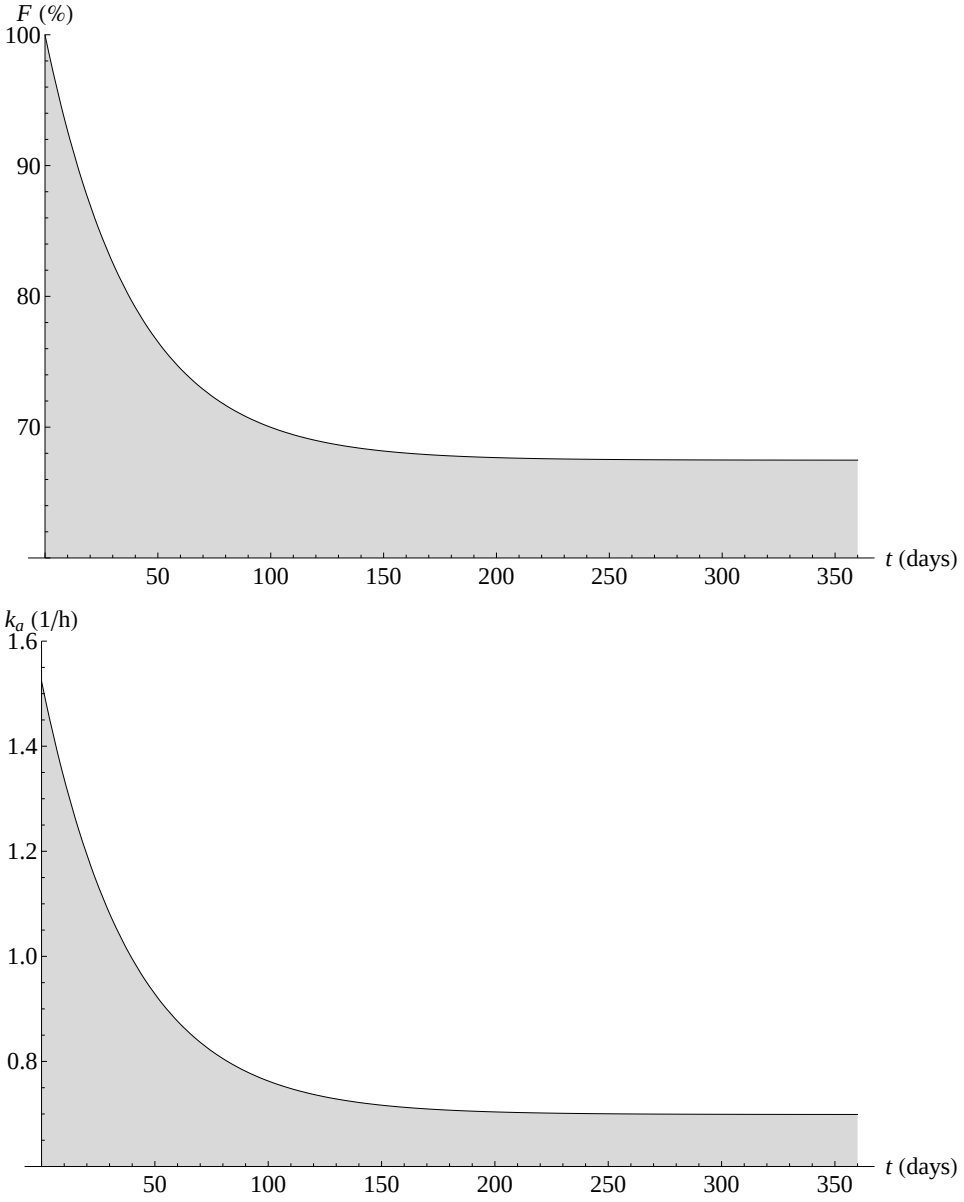

Figure 7.3: Decrease in apparent bioavailability F (*top*) and absorption k_a (*bottom*) over time.

study at Day 1. Using the respective estimates, both models have then been simulated against the data that were used in the final model, stratified on the different group of months (Day 1, Months 1 to 3, Months 5 to 6, and Months 11 and above, according to Table 6.2). In all sub-plots, black dots are the true observations, and the lines are the 50th (solid), 5th (dashed lower) and 95th (dashed upper) percentiles of these observations in each of the different time-intervals, comprising the 90% prediction interval. The shaded areas are the 95% confidence intervals of the corresponding percentiles for the simulated data (i.e., the predictions made by each model). In a perfect model the dashed lines would go in the middle of the respective light-gray

area and the solid line (the median) would go in the middle of the dark-gray area. Except at Day 1, for the VPC in Figure 7.5, the lines are clearly below the respective predicted confidence intervals. I.e., not using any time-effects will cause a large over-prediction from the model.

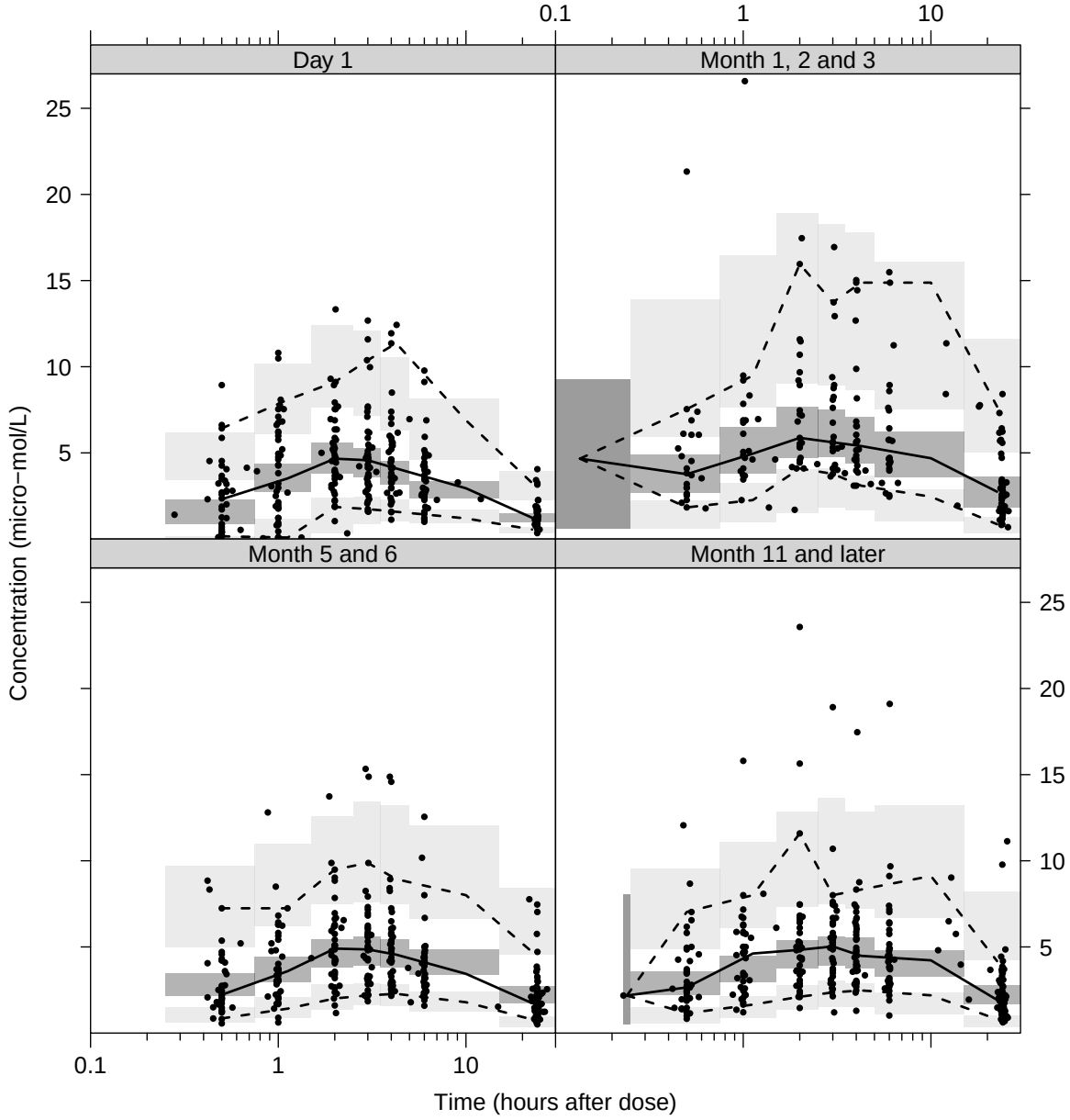

Figure 7.4: VPC for the final model (without the liver metastasis covariate).

To investigate compliance, pre-dose concentrations were compared to the maximum concentration for each rich occasion. Only one occasion in one subject where found where non-compliance may be suspected, since the pre-dose concentration was higher than all observations during the full course.

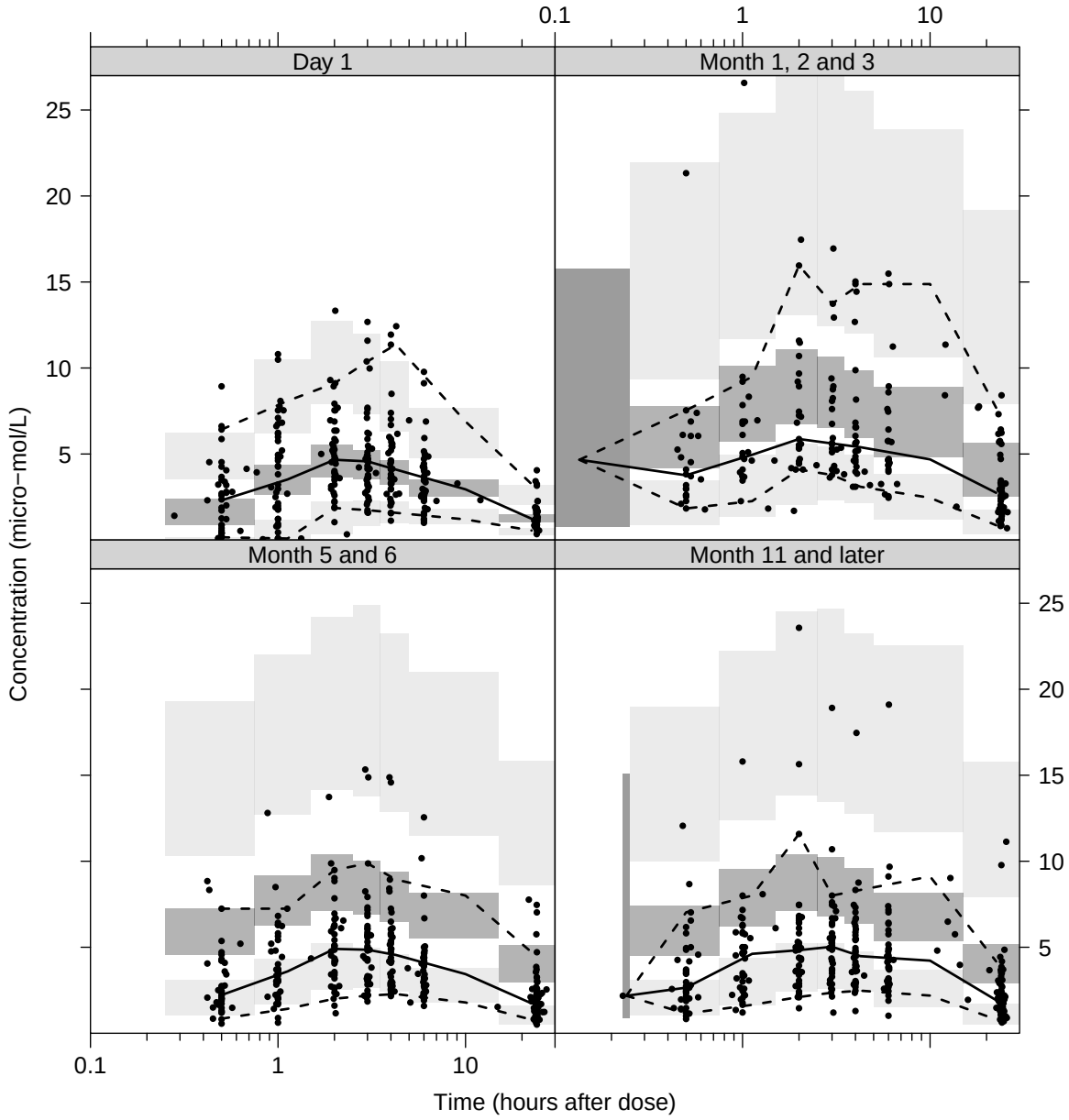

Figure 7.5: VPC for a model where the time dependency in F and k_a has been removed, and where parameters have been estimated from the rich occasions at Day 1.

7.3.3 Covariate analysis

For sampling occasions with missing information on body weight (WT), data was interpolated linearly between occasions, or extrapolated for WT missing at the start or end of the study period, from the specific patient. For patients completely missing data on body weight data was imputed by first taking the average within each patient and then the median of the average values, and stratify on sex. WT on CL gave a significant drop in OFV (Table 7.5, model no 8), but was omitted in the final model because of too much data imputation.

Volume of liver metastasis (LIVM) ranged from 0.68 to 1800 cm^3 (median 5.8 cm^3)

and the metastasis/liver volume ratio (LIVR), ranged from 0.042 to 61% (median 0.42%. Subjects not having liver metastasis were assigned LIVM = 0 and LIVR = 0 for all observations. The dichotomous covariate LIV was used to indicate whether a subject had liver metastasis (LIV = 1) or not (LIV = 0). Imatinib observations lacking information on LIVM and LIVR that belonged to subjects with metastasis were excluded.

Only the size (LIVM) of liver metastasis (model no 11) prevailed as a significant covariate ($p < 0.01$) when combined with other significant covariates (model no 19 and 20). The decrease in CL affected by LIVM could not be associated to the time dependency (models no 17 and 18). The predicted decrease in CL implies that for every 100 cm^3 increase in metastasis volume CL is decreased by almost 4%. However, for most subjects the metastasis will have very small effect on CL, considering the median value of LIVM in the study group.

Table 7.5: Time and covariate effects on the imatinib population PK-model

No	Time effect	Covariate effect	ΔOFV	Δd.f.[c]
1	-	-	246.4	-3
2	-	$CL \cdot (1 - \theta_{cov} \cdot \text{LIVM})$	228.0	-2
3	CL	-	168.7	-1
4	k_a	-	94.4	-1
5	F	-	42.9	-1
6	CL, k_a	-	4.3	0
7[a]	F, k_a	-	0	0
8	F, k_a	$CL \cdot (\text{WT}_{ind}/\text{WT}_{median})^{\theta_{cov}}$	-13.9	1
9	F, k_a	$V_{central} \cdot (\text{WT}_{ind}/\text{WT}_{median})^{\theta_{cov}}$	-0.3	1
10	F, k_a	$CL \cdot (1 - \theta_{cov} \cdot \text{LIV})$, LIV = 0/1	-0.4	1
11	F, k_a	$CL \cdot (1 - \theta_{cov} \cdot \text{LIVM})$	-21.8	1
12	F, k_a	$V_{central} \cdot (1 - \theta_{cov} \cdot \text{LIVM})$	-0.1	1
13	F, k_a	$F \cdot (1 - \theta_{cov} \cdot \text{LIVM})$	-7.1	1
14	F, k_a	$CL \cdot (1 - \theta_{cov} \cdot \text{LIVR})$	-11	1
15	F, k_a	$V_{central} \cdot (1 - \theta_{cov} \cdot \text{LIVR})$	-0.1	1
16	F, k_a	$F \cdot (1 - \theta_{cov} \cdot \text{LIVR})$	-1.7	1
17	F[b], k_a	$F \cdot \left(1 - \beta_F \cdot (1 - \theta_{cov} \cdot \text{LIVM}) \cdot e^{-\lambda \cdot \text{TIME}/24}\right)$	0	1
18	F[b], k_a	$F \cdot \left(1 - \beta_F \cdot e^{-\lambda \cdot \text{TIME}/24 \cdot (1 - \theta_{cov} \cdot \text{LIVM})}\right)$	-0.1	1
19	F, k_a	$CL \cdot (1 - \theta_{cov_1} \cdot \text{LIVM})$, $F \cdot (1 - \theta_{cov_2} \cdot \text{LIVM})$	-21.8	2
20	F, k_a	$CL \cdot (1 - \theta_{cov_1} \cdot \text{LIVM}) \cdot (1 - \theta_{cov_2} \cdot \text{LIVR})$	-24.1	2

[a] Model no 7 is considered to be the reference model w.r.t. OFV and d.f.

[b] Covariate effect integrated in time effect for F

[c] Δd.f. is the difference in number of degrees of freedom

7.4 Paper IV

The aim of Paper IV was to develop a pharmacokinetic model, "bottom-up". Instead of building a model based on patient data and try to explain mechanisms on a cellular level ("top-down"), development started with the cellular level, and the model was then scaled up to mimic the relevant parts of a human body as far as possible. This way, mechanisms potentially causing pharmacokinetic variability can be explicitly investigated. According to the final model, the main metabolite of paclitaxel was relatively largely affected also by small changes, while this was not the case for paclitaxel itself.

7.4.1 Model development and constrained optimization

A semi-physiologically based pharmacokinetic model for paclitaxel and metabolites was developed by using the intracellular pharmacokinetic model described by Kuh et al. [49] and Jang et al. [41] as a starting point. The model was up-scaled and extended to include three physiological compartments; systemic plasma, liver plasma and liver tissue, and one output compartment, similar to the framework presented by Sirianni and Pang [78]. Binding of paclitaxel and metabolites to plasma proteins and Cremophor EL was described according to the relations between total and unbound concentrations that have been used in population pharmacokinetic models [35, 38]. An extensive literature study was conducted to find reasonable parameter estimates to use for the model structure.

Constrained optimization was used to adjust the parameters so that concentration ratios between metabolites and paclitaxel in systemic plasma, and amount ratios between metabolites and paclitaxel in the output compartment were clinically reasonable and in correspondence with Paper II and the findings by Walle et al. [91]. A simulation of the final model, based on a three-hour infusion and using the estimates from the constrained optimization, is shown in Figure 7.6, with total concentrations (left) and unbound concentrations (right) of paclitaxel and its metabolites. Total concentrations are in the range of what has been clinically observed [14, 35, 36, 37, 43, 47]. Notably for paclitaxel, both total and unbound concentrations have two distinct phases, with a very flat second phase before the of infusion ($t = 3$). In Figure 7.6, right panel, it is also clear that the curve describing unbound concentrations for paclitaxel have its maximum, not at the end of infusion but at the beginning of the flat phase. All these characteristics are atypical in clinical studies [14, 35, 47], and are most likely a result of the restricted compartmental space. Previously developed population pharmacokinetic models of paclitaxel have used two or three compartments to describe the distribution of the parent drug, but these cannot be used in the current model

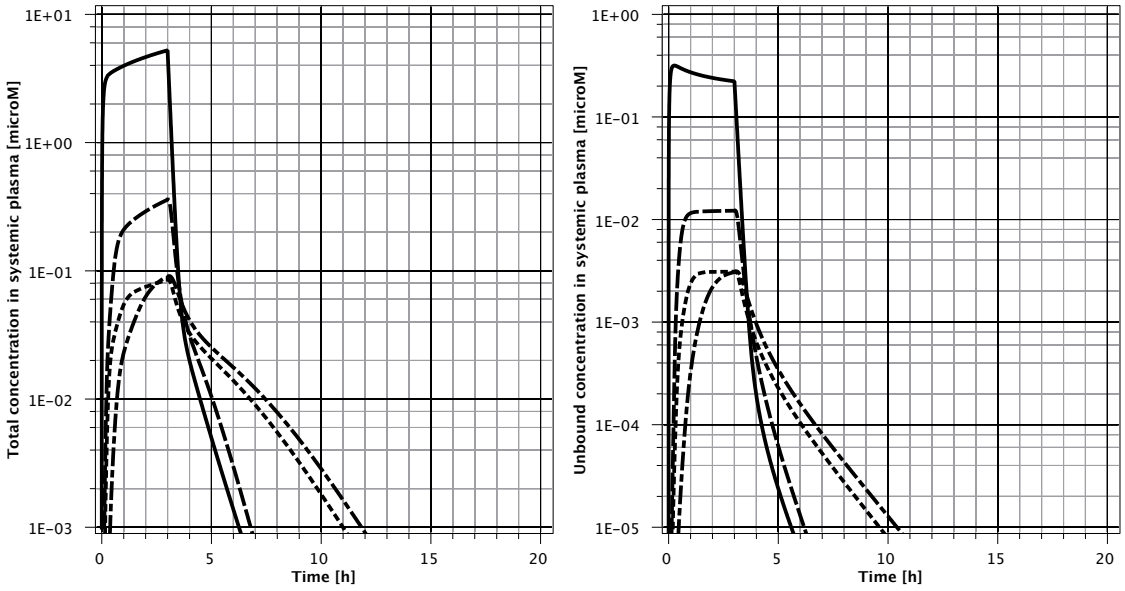

Figure 7.6: Simulations from the final model of total concentrations (*left*) and unbound concentrations (*right*) in systemic plasma of paclitaxel (solid), 6α-hydroxypaclitaxel (dashed), p-3'-hydroxypaclitaxel (dotted) and 6α-, p-3'-dihydroxypaclitaxel (dash-dotted).

since their estimates for distribution volumes and compartmental flows depend on unbound concentrations [35, 36, 37], or that they do not explicitly account for drug binding [43, 47]. To test the hypothesis of a restricted compartmental space, a simulation experiment using a ten times higher systemic plasma volume was performed, and is shown in Figure 7.7, with total concentrations (left) and unbound concentrations (left). By comparing Figures 7.6 and 7.7, it is apparent that while total paclitaxel concentrations no longer have a visible break-point between the two phases, the curve describing unbound concentrations have lost the initial peak, hence both curves show a more similar appearance to the real clinical situation during the time for infusion [35].

7.4.2 Dynamic sensitivity analysis

Influence of the transporters OATP and ABCB1, and the metabolizing enzymes CYP2C8 and CYP3A4, on concentrations and amounts was investigated using dynamic sensitivity analysis [39, 90, 96]. According to the semi-physiologically based pharmacokinetic model, metabolites were far more sensitive to changes in the metabolic pathway than the parent drug. The predicted change in concentration from a 10% decrease in different $GE^{V_{max}}$ at $t = 3$ hours, where the final model is using:

$$V_{max} = GE^{V_{max}} \cdot V_{max},\ GE^{V_{max}} = 1 \tag{7.5}$$

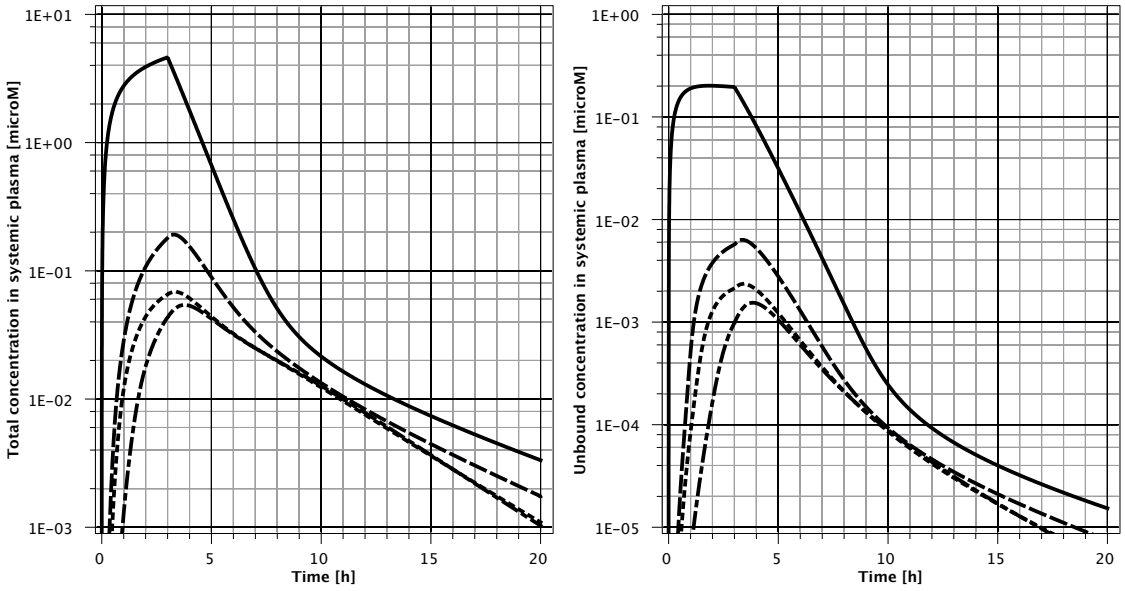

Figure 7.7: Simulation from a model using a ten times larger systemic plasma volume than the final model, with total concentrations (*left*) and unbound concentrations (*right*) in systemic plasma of paclitaxel (solid), 6α-hydroxypaclitaxel (dashed), p-3'-hydroxypaclitaxel (dotted) and 6α-, p-3'-dihydroxypaclitaxel (dash-dotted).

is given by the upper two rows in Table 7.6. By using dynamic sensitivity analysis on the alternative model with a ten times larger systemic plasma volume, the consistency of the results can be tested, and are presented in the lower two rows of Table 7.6. Results for the final model and the model with a ten times higher systemic plasma

Table 7.6: Change in total concentration of paclitaxel and 6α-hydroxypaclitaxel from a 10% decrease in different $GE^{V_{max}}$ in systemic plasma

Variable[a]	$GE^{V_{max}}_{OATP} = 0.9$	$GE^{V_{max}}_{2C8} = 0.9$	$GE^{V_{max}}_{3A4} = 0.9$	$GE^{V_{max}}_{ABC} = 0.9$
$x_1(3)$	2.3%	0.2%	0.1%	0.0%
$x_4(3)$	5.0%	-9.4%	6.7%	34.0%
$x_1(3, V_{SysPl\times 10})$	1.8%	0.1%	0.0%	0.0%
$x_4(3, V_{SysPl\times 10})$	2.3%	-6.5%	4.3%	21.6%

[a] $x_1(3)$: total paclitaxel concentration in systemic plasma at $t = 3$ hours; $x_4(3)$: total 6α-hydroxypaclitaxel concentration in systemic plasma at $t = 3$ hours; $x_1(3, V_{SysPl\times 10})$: total paclitaxel concentration in systemic plasma at $t = 3$ hours using a ten times larger systemic plasma volume; $x_4(3, V_{SysPl\times 10})$: total 6$\alpha$-hydroxypaclitaxel concentration in systemic plasma at $t = 3$ hours using a ten times larger systemic plasma volume

volume are consistent, albeit the later model is in general less affected by the 10% decrease. By comparing the peaks of total concentration of paclitaxel between the two models, and their respective sensitivity for $GE^{V_{max}}_{OATP}$, it is apparent in Figure 7.8, that the peak ratio (at approximately three hours) for the sensitivity curves (right) is larger than the peak ratio for the concentration curves (left). Notably, the model

with the ten times larger systemic plasma volume shows a different shape also for the sensitivity plot. In conclusion, comparing the change in AUC, in a similar way to what is done in Paper I, instead of concentration at $t = 3$, may be a better measure when testing consistency for the sensitivity analysis over different parameter values.

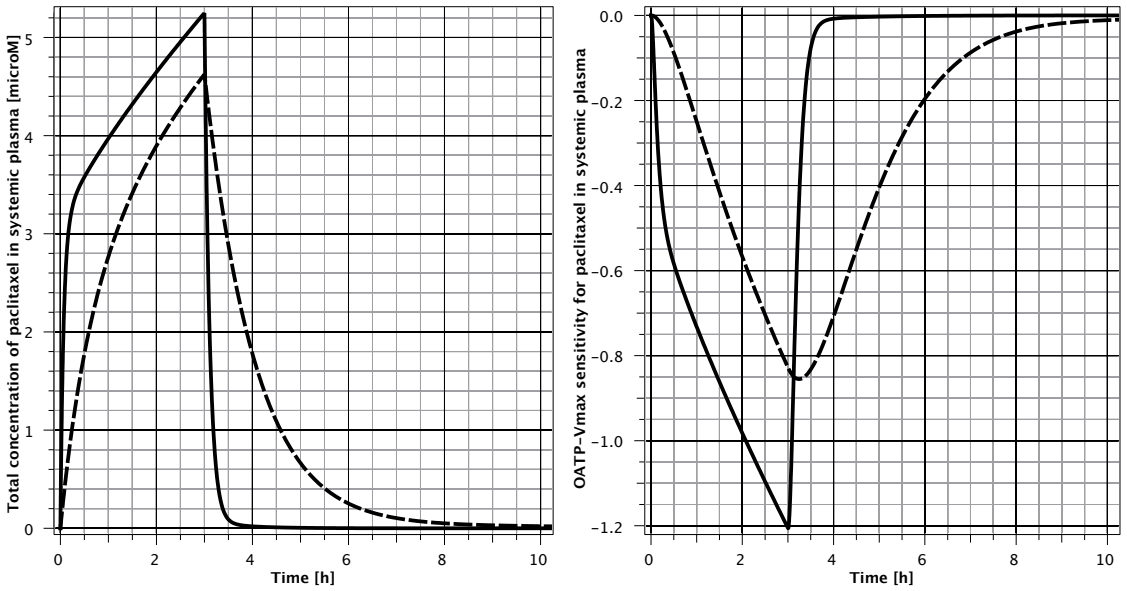

Figure 7.8: Total paclitaxel concentrations (*left*) and sensitivity in $GE^{V_{max}}$ for OATP (*right*), for the final model (solid) and the model with a ten times larger systemic plasma volume (dashed).

Overall, the results from the dynamic sensitivity analysis are in correspondence with observations from clinical studies. Of the two large large population pharmacokinetic studies looking at potential associations between genetic polymorphisms and paclitaxel kinetics, only Bergmann et al. [6] reported a significant finding in a population of 93 women, in which carriers of CYP2C8*3 had 11% lower clearance than non-carriers. Henningsson et al. [37] did not find any significant associations of CYP2C8, CYP3A4, CYP3A5, or ABCB1 in a much more heterogenous population of 97 men and women. While none of the larger studies investigated associations between polymorphisms and metabolites, the semi-physiologically based model supports the results from Paper II, where polymorphisms for the ABCB1 transporter showed a significant association to clearance of 6α-hydroxypaclitaxel. From Table 7.6 it is evident that the influence of ABCB1 on 6α-hydroxypaclitaxel is the most sensitive pathway according to the model. This could mean that this particular association may be the most apparent one in a clinical study.

8 Conclusions

Specific conclusions for the work in this thesis can be summarized as follows:

- Plasma concentrations of total paclitaxel can be used in pharmacokinetic modelling to predict the relation between total and unbound drug. This is important since only unbound drug is subject to membrane-protein transport and enzymatic metabolism.
- The solubilizer Cremophor EL seems to have a strong effect on the kinetics of paclitaxel hydroxymetabolites. Clearance of predicted unbound concentrations of the main metabolite 6α-hydroxypaclitaxel indicates an association with genetic polymorphisms in the ABCB1 gene.
- The pharmacokinetics for long-term treatment of gastrointestinal stromal tumour with imatinib is best described using a model with absorption delay and time dependent apparent bioavailability and absorption rate. Patients with considerable liver metastasis may have reduced drug clearance.
- The developed semi-physiologically based pharmacokinetic model for paclitaxel predicts systemic plasma concentrations of the metabolite 6α-hydroxypaclitaxel to be sensitive to changes in ABCB1 transport capacity.

Considering the overall aim of the thesis in relation to the conclusions:

Even for studies relatively rich in samples and subjects, geno- and phenotype covariates have little effect on the model fit compared to effects from drug binding or treatment duration. Hence, in order to individualize drug therapy, modelling may have to be moved to a lower level of detail, while keeping the perspective on the whole human body, as proposed by for instance Aarons [1]. Already, it may in general be difficult to investigate all important properties of a specific system due to limitations in data. Moving to an even more detailed level would therefore increase the need for methods that can combine physiologically-based models with molecular models, and previously developed models with new data.

Populärvetenskaplig sammanfattning

Farmakokinetisk variabilitet i en population kan sägas vara variationen mellan individernas blodplasmakoncentrationer av ett visst läkemedel. Denna variation kan till exempel orsakas av skillnader i gener som kodar för transportproteiner och enzymer, mängden kroppsfett, ålder, kön, diet eller patientens sjukdomstillstånd. För cancerläkemedel kan kombinationen av en hög variabilitet och ett så kallad smalt terapeutiskt fönster, d.v.s. skillnaden mellan en ineffektiv och en skadlig dos är liten, orsaka farliga biverkningar med ytterligare lidande som följd för den redan drabbade patienten och med höga kostnader för samhället.

Arbetet i denna avhandling syftar till att utforska möjligheterna till att individualisera behandling av två specifika cancerläkemedel, paklitaxel och imatinib, genom att utveckla matematiska modeller för att undersöka deras farmakokinetiska variabilitet.

Delarbete I syftade till att jämföra två publicerade farmakokinetiska modeller för paklitaxel. Den första modellen baseras endast på totala paklitaxelkoncentrationer, medan den andra som är en mer mekanistiskt trolig modell baseras normalt på både totala och obundna paklitaxelkoncentrationer, och även på koncentrationerna av lösningsmedlet Cremophor EL. Mer specifikt var syftet att undersöka om den mekanistiska modellen kan användas även om bara totala paklitaxelkoncentrationer finns tillgängliga. Resultaten visade att så var fallet och att det därmed är möjligt att utifrån totala koncentrationer beskriva hur obundna koncentrationer rör sig i kroppen. Detta är viktigt eftersom endast obundet läkemedel kan transporteras obehindrat eller brytas ned i levern, och därmed kan sägas vara närmre kopplat till den farmakokinetiska variabiliteten.

Delarbete II syftade till att utveckla en farmakokinetisk modell för paklitaxel och dess metaboliter med hjälp av data från en klinisk studie bestående av trettiotre kvinnor som fick cellgiftsbehandling för äggstockscancer. Delarbetet visade att liksom läkemedlet själv påverkas troligen också två av läkemedelsmetaboliterna till hög grad av lösningsmedlet Cremophor EL. Det visade sig också att den huvudsakliga

metaboliten verkar påverkas av vissa genetiska mutationer i ett så kallad transportprotein. Båda resultaten kan vara viktiga om det i framtiden visar sig att även metaboliterna kan orsaka biverkningar.

Delarbete III syftade till att utveckla en farmakokinetisk modell för imatinib genom att använda data från en klinisk studie med femtio män och kvinnor som fick långtidsbehandling för gastrointestinal stromacellstumör. Målet var att undersöka om det fanns en trend till minskade plasmakoncentrationer under behandlingstiden, samt att undersöka om läkemedelsnedbrytningen påverkades av om cancern hade spritt sig till levern (levermetastaser). Enligt modellen visade det sig att både den mängd läkemedel som absorberas av kroppen och den hastighet med vilket läkemedlet absorberas minskade väsentligt under behandlingstiden. Det visade sig också att patienter med väldigt stora levermetastaser hade minskad nedbrytning av läkemedlet.

Delarbete IV syftade till att utveckla en fysiologisk farmakokinetisk modell genom att utgå från en matematisk modell på cellnivå och sedan skala upp denna, istället för att som i Delarbeten I och II bygga en modell baserad på patientdata. På detta sätt kan de mekanismer som styr transport och nedbrytning av läkemedlet studeras noggrant genom datorsimuleringar. Enligt den slutliga modellen påverkades paklitaxel nästan inte alls av variationer under simuleringarna. Däremot påverkades den huvudsakliga metaboliten av variationer i det transportprotein som även framkom i Delarbete II.

Tack

Arbetet med den här avhandlingen påbörjades som ett samarbete mellan Linköpings universitet och MathCore Enginering. Det återupptogs på Karolinska Institutet och kunde avslutas med hjälp av Uppsala universitet och Erasmus Medical Center. Med så många parter involverade finns det självklart också många att personer att tacka.

Till följande vill jag säga:

Jan-Eric Litton, min huvudhandledare på Karolinska Institutet, tack för din uppmuntran att slutföra mitt avhandlingsarbete och för att du gav mig chansen att göra detta. Utan din tillit hade det inte varit möjligt!

Min bihandledare *Henrik Green*, tack för att du introducerade mig till farmakokinetik, för att jag fick ta del av din forskning och för ett gott samarbete. Du har varit en vän och en mentor under hela resans gång!

Min bihandledare *Lena Friberg*, tack för att du tog dig på rollen som min handledare, för ditt outtömliga förråd av idéer och stora tålamod. Du är en klippa!

Min tidigare huvudhandledare *Peter Fritzon*, tack för att du gav mig möjligheten att doktorera och själv forma mitt avhandlingsarbete!

Min bihandledare *Jan Brugård*, *Peter Aronsson*, *Daniel Hedberg*, *Katalin Bunus* och *MathCore*, tack för all hjälp med idéer, mjukvara och administration. Genom kopplingen till företaget har jag även fått viss förståelse för hur det funkar "där ute". Ovärderligt!

Min mentor *Sören Wahlund*, tack för alla våra samtal, för att du har delat med dig av din stora erfarenhet av livet, ledarskap och coachning som hjälpt mig att förstå mig själv bättre. Jag kommer sakna våra möten!

Lena Lewin och *Forskarskolan i Medicinsk Bioinformatik*, tack för finansiering av doktorandstudierna!

Karel Eechoute och mina övriga medförfattare i det tredje delarbetet, tack för ett gott samarbete!

Min bihandledare *Sven Sandin*, tack för våra samtal och för att du fick mig att se min forskning från ett annat perspektiv.

Curt Peterson och *Malin Lindqvist* på Hälsouniversitetet i Linköping, tack för ert stöd och ett gott samarbete under första tiden av mitt avhandlingsarbete.

Mats Karlsson, *Joakim Nyberg* och *farmakometrigruppen* på BMC i Uppsala, tack för att jag alltid har känt mig välkommen och för att ni har tagit er tid med mina frågor.

Mina kära vänner och meddoktorander, *Adina*, *Alexander*, *Christina*, *Iffat*, *Karin*, *Lisa*, *Lovisa*, *Maria*, *Miriam*, *Sara*, *Stephanie*, *Therese* och *Thomas*, tack för alla fikastunder, allt roligt, och för vänskap bortom MEBs väggar!

Mina kollegor i anslutning till arbetet med BBMRI, *Loreana Norlin*, *Sofie Petersson*, *Maria Anderberg*, *Roxana Martinez*, *Lisen Arnheim Dahlström*, *Sanela Kurtovic*, *Mikael Eriksson*, *Joakim Galli*, *Ann-Sofie Lundin*, *Mariam Lashkariani*, *Mark Divers* och *Connie Nordlund*, tack för en fantastisk arbetsatmosfär, alla trevliga fikastunder och för ert tålamod med min forskning.

Övriga nuvarande och före detta MEB:are, tack för att ni gör MEB till en så bra arbetsplats!

Anders, *John*, *Mattias*, *Rolle*, *Kristian Sandahl* och *PELAB*-gruppen, tack för doktorandtiden i Linköping!

Axel, *Åsa* och *Anna*, tack för att ni är såna fantastiska vänner!

Till sist vill jag tacka min familj, *Carin*, *Gunnar*, *Marcus*, *Magnus*, *Anna*, *Emma*, *Philip* och *Julia*, jag hade aldrig klarat den här resan utan er. Tack för att ni finns!

References

[1] L. Aarons. Physiologically based pharmacokinetic modelling: a sound mechanistic basis is needed. *Br J Clin Pharmacol*, 60:581–583, Dec 2005.

[2] G.D. Aletti, M.M. Gallenberg, W.A. Cliby, A. Jatoi, and L.C. Hartmann. Current management strategies for ovarian cancer. *Mayo Clin. Proc.*, 82(6):751–770, 2007.

[3] T. Barnes and D. Reinke. Practical management of imatinib in gastrointestinal stromal tumors. *Clin J Oncol Nurs*, 15:533–545, Oct 2011.

[4] S. Beal, L.B. Sheiner, A. Boeckmann, and R.J. Bauer. *NONMEM User's Guides (1989-2009)*. Icon Development Solutions, Ellicott City, MD, USA, 2009.

[5] J.M. Berg, J.L Tymoczko, and L. Stryer. *Biochemistry*. W.H. Freeman and Company, New York, USA, 5th edition, 2003.

[6] T. K. Bergmann, C. Brasch-Andersen, H. Green, M. Mirza, R. S. Pedersen, F. Nielsen, K. Skougaard, J. Wihl, N. Keldsen, P. Damkier, L. E. Friberg, C. Peterson, W. Vach, M. O. Karlsson, and K. Brosen. Impact of CYP2C8*3 on paclitaxel clearance: a population pharmacokinetic and pharmacogenomic study in 93 patients with ovarian cancer. *Pharmacogenomics J.*, 11:113–120, Apr 2011.

[7] J. H. Borovicka, C. Calahan, M. Gandhi, T. S. Abraham, M. J. Kwasny, A. C. Haley, D. P. West, and M. E. Lacouture. Economic burden of dermatologic adverse events induced by molecularly targeted cancer agents. *Arch Dermatol*, 147:1403–1409, Dec 2011.

[8] T.M. Bosch, A.D. Huitema, V.D. Doodeman, R. Jansen, E. Witteveen, W.M. Smit, R.L. Jansen, C.M. van Herpen, M. Soesan, J.H. Beijnen, and J.H. Schellens. Pharmacogenetic screening of CYP3A and ABCB1 in relation to population pharmacokinetics of docetaxel. *Clin. Cancer Res.*, 12(19):5786–5793, 2006.

[9] Kenneth P. Burnham and David R. Anderson. *Model Selection and Multi-Model Inference*. Springer-Verlag, Lund, Sweden, 2nd edition, 2002.

[10] M. V. Caram and S. M. Schuetze. Advanced or metastatic gastrointestinal stromal tumors: systemic treatment options. *J Surg Oncol*, 104:888–895, Dec 2011.

[11] G. Cedersund. *Core-box Modelling – Theoretical Contributions and Applications to Glucose Homeostasis Related Systems*. Phd thesis, Department of Signals and Systems, Chalmers University of Technology, Göteborg, Sweden, 2006.

[12] C. L. Corless, C. M. Barnett, and M. C. Heinrich. Gastrointestinal stromal tumours: origin and molecular oncology. *Nat. Rev. Cancer*, 11:865–878, 2011.

[13] T. Cresteil, B. Monsarrat, J. Dubois, M. Sonnier, P. Alvinerie, and F. Gueritte. Regioselective metabolism of taxoids by human CYP3A4 and 2C8: structure-activity relationship. *Drug Metab. Dispos.*, 30:438–445, Apr 2002.

[14] M. Czejka, J. Schueller, H. Schnait, B. Springer, and I. Eder. Clinical pharmacokinetics and metabolism of paclitaxel after a three-hour infusion: comparison of two preparations. *J Oncol Pharm Pract*, 9:129–136, 2003.

[15] C. Delbaldo, E. Chatelut, M. Re, A. Deroussent, S. Seronie-Vivien, A. Jambu, P. Berthaud, A. Le Cesne, J. Y. Blay, and G. Vassal. Pharmacokinetic-pharmacodynamic relationships of imatinib and its main metabolite in patients with advanced gastrointestinal stromal tumors. *Clin. Cancer Res.*, 12:6073–6078, Oct 2006.

[16] L. Edelstein-Keshet. *Mathematical Models in Biology.* McGraw-Hill, New York, USA, 1st edition, 1988.

[17] K. Eechoute, A. Sparreboom, H. Burger, R. M. Franke, G. Schiavon, J. Verweij, W. J. Loos, E. A. Wiemer, and R. H. Mathijssen. Drug transporters and imatinib treatment: implications for clinical practice. *Clin. Cancer Res.*, 17:406–415, Feb 2011.

[18] P. Fritzson. *Principles of Object-Oriented Modeling and Simulation with Modelica 2.1.* IEEE Press, Wiley-Interscience, Piscataway, NJ, USA, 1st edition, 2004.

[19] P. Fritzson, P. Aronsson, H. Lundvall, K. Nyström, A. Pop, L. Saldamli, and D. Broman. The OpenModelica Modeling, Simulation, and Software Development Environment. *Simulation News Europe*, 44/45:8–16, 2005.

[20] C. Gambacorti-Passerini. Part I: Milestones in personalised medicine–imatinib. *Lancet Oncol.*, 9:600, Jun 2008.

[21] H. Gelderblom, J. Verweij, K. Nooter, and A. Sparreboom. Cremophor EL: the drawbacks and advantages of vehicle selection for drug formulation. *Eur. J. Cancer*, 37:1590–1598, Sep 2001.

[22] Andrew Gelman, Frederic Bois, and Jiming Jiang. Physiological pharmacokinetic analysis using population modeling and informative prior distributions. *Journal of the American Statistical Association*, 91:1400–1412, 1996.

[23] L Gianni, C. M. Kearns, A. Giani, G. Capri, L. Vigano, A. Locatelli, G. Bonadonna, and M. J. Egorin. Nonlinear pharmacokinetics and metabolism of paclitaxel and its pharmacokinetic/pharmacodynamic relationships in humans. *J. Clin. Oncol.*, 13:180–190, 1995.

[24] P.O. Gisleskog, M.O. Karlsson, and S.L. Beal. Use of prior information to stabilize a population data analysis. *J. Pharmacokinet. Pharmacodyn.*, 29(5-6): 473–505, 2002.

[25] H. Green, P. Soderkvist, P. Rosenberg, G. Horvath, and C. Peterson. mdr-1 single nucleotide polymorphisms in ovarian cancer tissue: G2677T/A correlates with response to paclitaxel chemotherapy. *Clin. Cancer Res.*, 12:854–859, Feb 2006.

[26] H. Green, K. Vretenbrant, B Norlander, and C Peterson. Measurement of paclitaxel and its metabolites in human plasma using liquid chromatography/ion trap mass spectrometry with a sonic spray ionization interface. *Rapid Commun Mass Spectrom.*, 20:2183–2189, 2006.

[27] H. Green, P. Soderkvist, P. Rosenberg, R. A. Mirghani, P. Rymark, E. A. Lundqvist, and C. Peterson. Pharmacogenetic studies of Paclitaxel in the treatment of ovarian cancer. *Basic Clin. Pharmacol. Toxicol.*, 104:130–137, Feb 2009.

[28] H. P. Gschwind, U. Pfaar, F. Waldmeier, M. Zollinger, C. Sayer, P. Zbinden, M. Hayes, R. Pokorny, M. Seiberling, M. Ben-Am, B. Peng, and G. Gross. Metabolism and disposition of imatinib mesylate in healthy volunteers. *Drug Metab. Dispos.*, 33:1503–1512, Oct 2005.

[29] J. W. Harris, A. Katki, L. W. Anderson, G. N. Chmurny, J. V. Paukstelis, and J. M. Collins. Isolation, structural determination, and biological activity of 6 alpha-hydroxytaxol, the principal human metabolite of taxol. *J. Med. Chem.*, 37:706–709, Mar 1994.

[30] J. W. Harris, A. Rahman, B. R. Kim, F. P. Guengerich, and J. M. Collins. Metabolism of taxol by human hepatic microsomes and liver slices: participation of cytochrome P450 3A4 and an unknown P450 enzyme. *Cancer Res.*, 54:4026–4035, Aug 1994.

[31] M.J. Hassett, A.J. O'Malley, J.R. Pakes, J.P. Newhouse, and C.C. Earle. Frequency and cost of chemotherapy-related serious adverse effects in a population sample of women with breast cancer. *J. Natl. Cancer Inst.*, 98(16):1108–1117, 2006.

[32] A. Heck. *Introduction to Maple.* Springer-Verlag, New York, NY, USA, 3rd edition, 2003.

[33] J.F. Hendrickx, H.J. Lemmens, and S.L. Shafer. Do distribution volumes and clearances relate to tissue volumes and blood flows? a computer simulation. *BMC Anesthesiol.*, 6(7), 2006.

[34] K.L. Hennenfent and R. Govindan. Novel formulations of taxanes: a review. Old wine in a new bottle? *Ann. Oncol.*, 17(5):735–749, 2006.

[35] A. Henningsson, M. O. Karlsson, L. Vigano, L. Gianni, J. Verweij, and A. Sparreboom. Mechanism-based pharmacokinetic model for paclitaxel. *J. Clin. Oncol.*, 19:4065–4073, Oct 2001.

[36] A. Henningsson, A. Sparreboom, M. Sandstrom, A. Freijs, R. Larsson, J. Bergh, P. Nygren, and M. O. Karlsson. Population pharmacokinetic modelling of unbound and total plasma concentrations of paclitaxel in cancer patients. *Eur. J. Cancer*, 39:1105–1114, May 2003.

[37] A. Henningsson, S. Marsh, W. J. Loos, M. O. Karlsson, A. Garsa, K. Mross, S. Mielke, L. Vigano, A. Locatelli, J. Verweij, A. Sparreboom, and H. L. McLeod. Association of CYP2C8, CYP3A4, CYP3A5, and ABCB1 polymorphisms with the pharmacokinetics of paclitaxel. *Clin. Cancer Res.*, 11:8097–8104, Nov 2005.

[38] A. Henningsson, A. Sparreboom, W. J. Loos, J. Verweij, M. Silvander, and M. O. Karlsson. Population pharmacokinetic model for Cremophor EL (Abstract). *PAGE*, 14:770, 2005.

[39] Alan C. Hindmarsh, Peter N. Brown, Keith E. Grant, Steven L. Lee, Radu Serban, Dan E. Shumaker, and Carol S. Woodward. SUNDIALS: Suite of nonlinear and differential/algebraic equation solvers. *ACM Transactions on Mathematical Software*, 31(3):363–396, Sep 2005.

[40] N. Holford. The Visual Predictive Check - Superiority to Standard Diagnostic (Rorschach) Plots (Abstract). *PAGE*, 14:738, 2005.

[41] S. H. Jang, M. G. Wientjes, and J. L. Au. Kinetics of P-glycoprotein-mediated efflux of paclitaxel. *J. Pharmacol. Exp. Ther.*, 298:1236–1242, Sep 2001.

[42] A. Jemal, F. Bray, M. M. Center, J. Ferlay, E. Ward, and D. Forman. Global cancer statistics. *CA Cancer J Clin*, 61:69–90, 2011.

[43] M. Joerger, A. D. Huitema, D. H. van den Bongard, J. H. Schellens, and J. H. Beijnen. Quantitative effect of gender, age, liver function, and body size on the population pharmacokinetics of Paclitaxel in patients with solid tumors. *Clin. Cancer Res.*, 12:2150–2157, Apr 2006.

[44] E. N. Jonsson and M. O. Karlsson. Xpose – an S-PLUS based population pharmacokinetic/pharmacodynamic model building aid for NONMEM. *Comput. Methods Programs Biomed.*, 58:51–64, 1999.

[45] I. Judson, P. Ma, B. Peng, J. Verweij, A. Racine, E. D. di Paola, M. van Glabbeke, S. Dimitrijevic, M. Scurr, H. Dumez, and A. van Oosterom. Imatinib pharmacokinetics in patients with gastrointestinal stromal tumour: a retrospective population pharmacokinetic study over time. EORTC Soft Tissue and Bone Sarcoma Group. *Cancer Chemother. Pharmacol.*, 55:379–386, Apr 2005.

[46] R.E. Kalman. A new approach to linear filtering and prediction problems. *Transactions of the ASME – Journal of Basic Engineering*, 82(Series D):35–45, 1960.

[47] M. O. Karlsson, V. Molnar, A. Freijs, P. Nygren, J. Bergh, and R. Larsson. Pharmacokinetic models for the saturable distribution of paclitaxel. *Drug Metab. Dispos.*, 27:1220–1223, Oct 1999.

[48] M.O. Karlsson and L.B. Sheiner. The importance of modeling interoccasion variability in population pharmacokinetic analyses. *J. Pharmacokinet. Biopharm.*, 21(6):735–750, 1993.

[49] H. J. Kuh, S. H. Jang, M. G. Wientjes, and J. L. Au. Computational model of intracellular pharmacokinetics of paclitaxel. *J. Pharmacol. Exp. Ther.*, 293: 761–770, Jun 2000.

[50] G. N. Kumar, J. E. Oatis, K. R. Thornburg, F. J. Heldrich, E. S. Hazard, and T. Walle. 6 alpha-Hydroxytaxol: isolation and identification of the major metabolite of taxol in human liver microsomes. *Drug Metab. Dispos.*, 22:177–179, 1994.

[51] M.C. Launay-Iliadis, R. Bruno, V. Cosson, J.C. Vergniol, D. Oulid-Aissa, M. Marty, M. Clavel, M. Aapro, N. Le Bail, and A. Iliadis. Population pharmacokinetics of docetaxel during phase I studies using nonlinear mixed-effect modeling and nonparametric maximum-likelihood estimation. *Cancer Chemother. Pharmacol.*, 37(1-2):47–54, 1995.

[52] L. Lindbom, P. Pihlgren, and E. N. Jonsson. PsN-Toolkit–a collection of computer intensive statistical methods for non-linear mixed effect modeling using NONMEM. *Comput Methods Programs Biomed*, 79:241–257, Sep 2005.

[53] L. Ljung. *System Identification: Theory for the User, second edition*. Prentice-Hall PTR, Upper Saddle River, NJ, USA, 2nd edition, 1999.

[54] Maplesoft, Waterloo Maple Inc. *Maple 10*. Maplesoft, Waterloo Maple Inc., Waterloo, ON, Canada, 2005.

[55] V.R Martin. Ovarian cancer: an overview of treatment options. *Clin. J. Oncol. Nurs.*, 11(2):201–207, 2007.

[56] D. Menon-Andersen, J. T. Mondick, B. Jayaraman, P. A. Thompson, S. M. Blaney, M. Bernstein, M. Bond, M. Champagne, M. J. Fossler, and J. S. Barrett. Population pharmacokinetics of imatinib mesylate and its metabolite in children and young adults. *Cancer Chemother. Pharmacol.*, 63:229–238, Jan 2009.

[57] R. A. Mirghani, U. Hellgren, P. A. Westerberg, O. Ericsson, L. Bertilsson, and L. L. Gustafsson. The roles of cytochrome P450 3A4 and 1A2 in the 3-hydroxylation of quinine in vivo. *Clin. Pharmacol. Ther.*, 66:454–460, Nov 1999.

[58] R. A. Mirghani, O. Ericsson, J. Cook, P. Yu, and L. L. Gustafsson. Simultaneous determination of quinine and four metabolites in plasma and urine by high-performance liquid chromatography. *J. Chromatogr. B Biomed. Sci. Appl.*, 754: 57–64, Apr 2001.

[59] M. Nakajima, Y. Fujiki, S. Kyo, T. Kanaya, M. Nakamura, Y. Maida, M. Tanaka, M. Inoue, and T. Yokoi. Pharmacokinetics of paclitaxel in ovarian cancer patients and genetic polymorphisms of CYP2C8, CYP3A4, and MDR1. *J Clin Pharmacol*, 45:674–682, Jun 2005.

[60] B. Nilsson, P. Bumming, J. M. Meis-Kindblom, A. Oden, A. Dortok, B. Gustavsson, K. Sablinska, and L. G. Kindblom. Gastrointestinal stromal tumors: the incidence, prevalence, clinical course, and prognostication in the preimatinib mesylate era–a population-based study in western Sweden. *Cancer*, 103:821–829, Feb 2005.

[61] B. Peng, C. Dutreix, G. Mehring, M. J. Hayes, M. Ben-Am, M. Seiberling, R. Pokorny, R. Capdeville, and P. Lloyd. Absolute bioavailability of imatinib (Glivec) orally versus intravenous infusion. *J Clin Pharmacol*, 44:158–162, Feb 2004.

[62] A. Petain, D. Kattygnarath, J. Azard, E. Chatelut, C. Delbaldo, B. Geoerger, M. Barrois, S. Seronie-Vivien, A. LeCesne, and G. Vassal. Population pharmacokinetics and pharmacogenetics of imatinib in children and adults. *Clin. Cancer Res.*, 14:7102–7109, Nov 2008.

[63] S. Pignata, L. Cannella, D. Leopardo, C. Pisano, G. S. Bruni, and G. Facchini. Chemotherapy in epithelial ovarian cancer. *Cancer Lett.*, 303:73–83, Apr 2011.

[64] D. Piszkiewicz. Letter: Micelle catalyzed reactions are models of enzyme catalyzed reactions which show positive homotropic interactions. *J. Am. Chem. Soc.*, 98:3053–3055, May 1976.

[65] D. Piszkiewicz. Positive cooperativity in micelle-catalyzed reactions. *J. Am. Chem. Soc.*, 99:1550–1557, Mar 1977.

[66] R Development Core Team. *R: A Language and Environment for Statistical Computing*. R Foundation for Statistical Computing, Vienna, Austria, 2007. URL `http://www.R-project.org`. ISBN 3-900051-07-0.

[67] A. Rahman, K. R. Korzekwa, J. Grogan, F. J. Gonzalez, and J. W. Harris. Selective biotransformation of taxol to 6 alpha-hydroxytaxol by human cytochrome P450 2C8. *Cancer Res.*, 54:5543–5546, Nov 1994.

[68] H.P. Rang, M.M Dale, J.M. Ritter, and P.K. Moore. *Pharmacology*. Churchill Livingstone, United Kingdom, 5th edition, 2003.

[69] J.F Ritt. *Differential Algebra*. American Mathematical Society, Providence, RI, USA, 1950. URL http://www.ams.org/online_bks/coll33/.

[70] E. K. Rowinsky and R. C. Donehower. Paclitaxel (taxol). *N. Engl. J. Med.*, 332: 1004–1014, Apr 1995.

[71] A. Russo, M. Autelitano, and L. Bisanti. Re: Frequency and cost of chemotherapy-related serious adverse effects in a population sample of women with breast cancer. *J. Natl. Cancer Inst.*, 98(24):1826–1827, 2006.

[72] R. M. Savic, D. M. Jonker, T. Kerbusch, and M. O. Karlsson. Implementation of a transit compartment model for describing drug absorption in pharmacokinetic studies. *J Pharmacokinet Pharmacodyn*, 34:711–726, Oct 2007.

[73] G. Schiavon, K. Eechoute, R. H. Mathijssen, P. de Bruijn, J. M. van der Bol, J. Verweij, S. Sleijfer, and W. J. Loos. Biliary Excretion of Imatinib and Its Active Metabolite CGP74588 During Severe Hepatic Dysfunction. *J Clin Pharmacol*, May 2011.

[74] P. B. Schiff, J. Fant, and S. B. Horwitz. Promotion of microtubule assembly in vitro by taxol. *Nature*, 277:665–667, Feb 1979.

[75] H. Schmidli, B. Peng, G. J. Riviere, R. Capdeville, M. Hensley, I. Gathmann, A. E. Bolton, and A. Racine-Poon. Population pharmacokinetics of imatinib mesylate in patients with chronic-phase chronic myeloid leukaemia: results of a phase III study. *Br J Clin Pharmacol*, 60:35–44, Jul 2005.

[76] A. Sedoglavic. A probabilistic algorithm to test local algebraic observability in polynomial time. *Journal of Symbolic Computation*, 33:735–755, 2002.

[77] I.H. Segel. *Enzyme kinetics : behavior and analysis of rapid equilibrium and steady state enzyme systems*. Wiley, New York, USA, 1975.

[78] G. L. Sirianni and K. S. Pang. Organ clearance concepts: new perspectives on old principles. *J Pharmacokinet Biopharm*, 25:449–470, Aug 1997.

[79] T. M. Sissung, K. Mross, S. M. Steinberg, D. Behringer, W. D. Figg, A. Sparreboom, and S. Mielke. Association of ABCB1 genotypes with paclitaxel-mediated peripheral neuropathy and neutropenia. *Eur. J. Cancer*, 42:2893–2896, Nov 2006.

[80] N. F. Smith, M. R. Acharya, N. Desai, W. D. Figg, and A. Sparreboom. Identification of OATP1B3 as a high-affinity hepatocellular transporter of paclitaxel. *Cancer Biol. Ther.*, 4:815–818, Aug 2005.

[81] D. S. Sonnichsen, C. A. Hurwitz, C. B. Pratt, J. J. Shuster, and M. V. Relling. Saturable pharmacokinetics and paclitaxel pharmacodynamics in children with solid tumors. *J. Clin. Oncol.*, 12:532–538, 1994.

[82] D. S. Sonnichsen, Q. Liu, E. G. Schuetz, J. D. Schuetz, A. Pappo, and M. V. Relling. Variability in human cytochrome P450 paclitaxel metabolism. *J. Pharmacol. Exp. Ther.*, 275:566–575, Nov 1995.

[83] M. E. Stokes, C. E. Muehlenbein, M. D. Marciniak, D. E. Faries, S. Motabar, T. W. Gillespie, J. Lipscomb, K. B. Knopf, and D. P. Buesching. Neutropenia-related costs in patients treated with first-line chemotherapy for advanced non-small cell lung cancer. *J Manag Care Pharm*, 15:669–682, Oct 2009.

[84] C.C. Sun, P.T. Ramirez, and D.C. Bodurka. Quality of life for patients with epithelial ovarian cancer. *Nat. Clin. Pract. Oncol.*, 4(1):18–29, 2007.

[85] T. Thigpen, A. duBois, J. McAlpine, P. DiSaia, K. Fujiwara, W. Hoskins, G. Kristensen, R. Mannel, M. Markman, J. Pfisterer, M. Quinn, N. Reed, A. M. Swart, J. Berek, N. Colombo, G. Freyer, D. Gallardo, M. Plante, A. Poveda, L. Rubinstein, M. Bacon, H. Kitchener, and G. C. Stuart. First-line therapy in ovarian cancer trials. *Int. J. Gynecol. Cancer*, 21:756–762, May 2011.

[86] C.W. Tornoe, J.L. Jacobsen, O. Pedersen, T. Hansen, and H. Madsen. Grey-box modelling of pharmacokinetic/pharmacodynamic systems. *J. Pharmacokinet. Pharmacodyn.*, 31(5):401–417, 2004.

[87] C.W. Tornoe, R.V. Overgaard, H. Agerso, H.A. Nielsen, H. Madsen, and E.N. Jonsson. Stochastic differential equations in NONMEM: implementation, application, and comparison with ordinary differential equations. *Pharm. Res.*, 22(8): 1247–1258, 2005.

[88] S. D. Undevia, G. Gomez-Abuin, and M. J. Ratain. Pharmacokinetic variability of anticancer agents. *Nat. Rev. Cancer*, 5:447–458, Jun 2005.

[89] N. P. van Erp, H. Gelderblom, M. O. Karlsson, J. Li, M. Zhao, J. Ouwerkerk, J. W. Nortier, H. J. Guchelaar, S. D. Baker, and A. Sparreboom. Influence of CYP3A4 inhibition on the steady-state pharmacokinetics of imatinib. *Clin. Cancer Res.*, 13:7394–7400, Dec 2007.

[90] A. Varma, M. Morbidelli, and H. Wu. *Parametric sensitivity in chemical systems.* Cambridge series in chemical engineering. Cambridge University Press, 1999. ISBN 9780521621717.

[91] T. Walle, U. K. Walle, G. N. Kumar, and K. N. Bhalla. Taxol metabolism and disposition in cancer patients. *Drug Metab. Dispos.*, 23:506–512, Apr 1995.

[92] Y. Wang. Derivation of various NONMEM estimation methods. *J. Pharmacokinet. Pharmacodyn.*, 34:575–593, 2007.

[93] N. Widmer, L. A. Decosterd, C. Csajka, S. Leyvraz, M. A. Duchosal, A. Rosselet, B. Rochat, C. B. Eap, H. Henry, J. Biollaz, and T. Buclin. Population pharmacokinetics of imatinib and the role of alpha-acid glycoprotein. *Br J Clin Pharmacol*, 62:97–112, Jul 2006.

[94] J. J. Wilkins, R. M. Savic, M. O. Karlsson, G. Langdon, H. McIlleron, G. Pillai, P. J. Smith, and U. S. Simonsson. Population pharmacokinetics of rifampin in pulmonary tuberculosis patients, including a semimechanistic model to describe variable absorption. *Antimicrob. Agents Chemother.*, 52:2138–2148, Jun 2008.

[95] Wolfram Research Inc. *Mathematica*. Wolfram Research Inc., Champaign, IL, USA, 2005.

[96] W. H. Wu, F. S. Wang, and M. S. Chang. Dynamic sensitivity analysis of biological systems. *BMC Bioinformatics*, 9 Suppl 12:S17, 2008.

[97] H. Yamaguchi, T. Hishinuma, N. Endo, H. Tsukamoto, Y. Kishikawa, M. Sato, Y. Murai, M. Hiratsuka, K. Ito, C. Okamura, N. Yaegashi, N. Suzuki, Y. Tomioka, and J. Goto. Genetic variation in ABCB1 influences paclitaxel pharmacokinetics in Japanese patients with ovarian cancer. *Int. J. Gynecol. Cancer*, 16:979–985, 2006.

[98] K. Zotos. Performance comparison of Maple and Mathematica. *Applied Mathematics and Computation*, 188:1426–1429, 2007.